



Cite this: *Nanoscale Horiz.*, 2020, 5, 1155

## Nano/microstructures of shape memory polymers: from materials to applications

Fenghua Zhang,<sup>a</sup> Yuliang Xia,<sup>a</sup> Yanju Liu<sup>b</sup> and Jinsong Leng<sup>id</sup>\*<sup>a</sup>

Shape memory polymers (SMPs) are macromolecules in which linear chains and crosslinking points play a key role in providing a shape memory effect. As smart polymers, SMPs have the ability to change shape, stiffness, size, and structure when exposed to external stimuli, leading to potential uses for SMPs throughout our daily lives in a diverse range of areas including the aerospace and automotive industries, robotics, biomedical engineering, smart textiles, and tactile devices. SMPs can be fabricated in many forms and sizes from the nanoscale to the macroscale, including nanofibers, nanoparticles, thin films, microfoams, and bulk devices. The introduction of nanostructure into SMPs can result in enhanced mechanical properties, unique structural color, specific surface area, and multiple functions. It is necessary to enhance the current understanding of the various nano/microstructures of SMPs and their fabrication, and to find suitable approaches for constructing SMP-based nano/microstructures for different applications. In this review, we summarize the current state of different SMP nano/microstructures, fabrication techniques, and applications, and give suggestions for their future development.

Received 28th April 2020,  
Accepted 1st June 2020

DOI: 10.1039/d0nh00246a

rsc.li/nanoscale-horizons

### 1. Introduction

Biological systems that integrate sensing, actuation, and control can serve as useful models for smart materials.<sup>1–3</sup> For example, the plant *Mimosa pudica* (Fig. 1) responds to an external stimulus and converts chemical signals into mechanical action. In the animal kingdom, chameleon skin exhibits smart behavior and provides protection against attack by changing color according to the surroundings. In practice, materials scientists have been

<sup>a</sup> National Key Laboratory of Science and Technology on Advanced Composites in Special Environments, Harbin Institute of Technology (HIT), Harbin 150080, P. R. China. E-mail: lengjs@hit.edu.cn

<sup>b</sup> Department of Astronautical Science and Mechanics, Harbin Institute of Technology (HIT), Harbin 150001, P. R. China



Fenghua Zhang

Fenghua Zhang is a lecturer at the Center for Smart Materials and Structures at Harbin Institute of Technology (HIT), China. She obtained her PhD degree in the field of materials at HIT in 2017. From 2014 to 2016, she as a visiting student did her research work at University of Cambridge supported by CSC. She has published more than 40 SCI scientific papers. Her research interests are focusing on shape memory polymers and their

composites, including shape memory polymers with nano/microstructures, 4D printed smart materials and structures for biomedical applications, stimuli methods and multifunctional composite materials.



Yuliang Xia

Yuliang Xia received his BS degree in materials chemistry in 2019 from Harbin Institute of Technology and now he is a PhD candidate under the supervision of Professor Jinsong Leng. He took an exchange internship in 2017 at Texas A&M University. In addition, he obtained the best student paper award at the SMART 2018 conference. Currently, his research focuses on the synthesis and optimization of shape memory intelligent

materials, as well as exploring their underlying mechanism and applications.

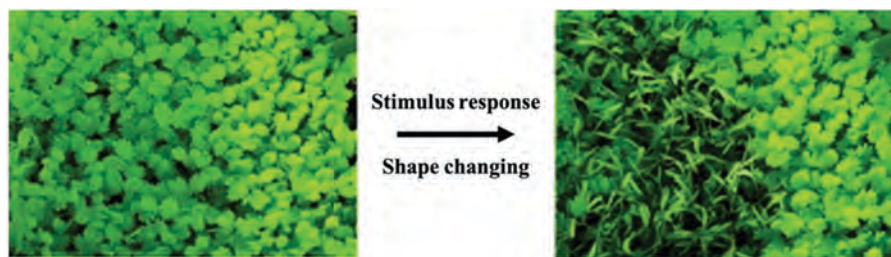


Fig. 1 Stimulus-responsive plant: *Mimosa pudica*.

able to mimic biology and artificially produce smart materials that behave in a similar way and respond to an even broader range of stimuli.<sup>4–6</sup>

Academic and industrial research on soft shape-changing materials is an active field of research that is receiving worldwide attention.<sup>7–9</sup> Shape memory polymers (SMPs) in particular exhibit excellent characteristics, as they can respond to external stimuli,<sup>10</sup> including heat,<sup>11</sup> light,<sup>12</sup> pH,<sup>13</sup> microwaves,<sup>14</sup> electrical and magnetic fields,<sup>15,16</sup> water,<sup>17</sup> pressure,<sup>18</sup> ultrasound,<sup>19</sup> and vapor,<sup>20</sup> leading to changes in their shape, size, strain, or stiffness.<sup>21</sup> Such characteristics promise numerous potential opportunities that make them of great interest to researchers, significantly promoting activity and investment in this area.

Recent advances in shape-changing materials have demonstrated the inherent potential of materials with flexible and tunable shapes,<sup>22–25</sup> and therefore SMPs are becoming increasingly well-known and are appearing in a diverse range of applications and environments.<sup>7,23,24</sup> High-performance loadbearing substructures of satellites, aircraft, and robots designed for structural efficiency have been developed to incorporate smart components to trigger folding, extending, and bending of components to add active functions.<sup>25–27</sup> In the industrial sector, a multitude of important novel practical applications are being developed, including smart clothes,<sup>28</sup>

self-healing systems,<sup>29</sup> anti-counterfeiting measures,<sup>30</sup> information carriers,<sup>31</sup> optical devices,<sup>32</sup> and biomedical devices.<sup>33,34</sup> In addition, 4D printing has been developed as a new fabrication technology, adding the extra dimension of time-dependent shape change to established 3D printing by enabling spatial variation of the material properties in each element of the printed component.<sup>35–37</sup> SMPs are an exemplar of active shape-changing materials that have seen rapid development in recent years and have led the way in terms of the nature and variety of material properties demonstrated.<sup>7,10,38–40</sup>

Nanotechnology is an interdisciplinary and comprehensive subject, which involves a wide range of modern science and technology. The preparation and research of nanomaterials are the basis of the whole of nanotechnology. Among them, nanophysics and nanochemistry are the theoretical basis of nanotechnology. Nanotechnology focuses on the design and manufacture of nanostructures, including nanofibers, nanoconstructions, nanofoams, nanopatterns, and nanoparticles, as shown in Fig. 2. When the structure is as small as the nanoscale, it may surpass or even be different from the macroscale structure in electronics, optics, mechanics and other aspects. Controllable nano/microstructures can be used to design and optimize the properties of materials at the nano/microscale, improving the performance of SMPs in various applications. Owing to the structural diversity, the correlations between the



**Yanju Liu**

*Yanju Liu is a professor in the Department of Aerospace Science and Mechanics at the Harbin Institute of Technology (HIT), China. From 1999 to 2003, she was a research fellow at Nanyang Technological University and Newcastle University. She was invited to serve as an associate editor of the journal of Smart Materials and Structures, a Committee Member of APCSNM, and a Committee Member of SAMPE. She is working on smart*

*materials and structures, including electrorheological and magnetorheological fluids, electroactive polymers, and shape memory polymers and their nanocomposites. She has authored or co-authored over 170 scientific papers in different journals.*



**Jinsong Leng**

*Jinsong Leng is a Cheung Kong Chair professor and Director of the Center for Smart Materials and Structures at Harbin Institute of Technology, China. His research interests cover shape memory polymers and their composites. He serves as the Vice President of International Committee on Composite Materials (ICCM). He is elected as the Foreign Member of Academia Europaea, Member of the European Academy of Science and*

*Arts, World Fellow of ICCM, Fellow of AAAS, Fellow of SPIE, Fellow of the Institute of Physics (IOP), Fellow of the Royal Aeronautical Society (RAeS), Fellow of IMMM and Associate Fellow of AIAA.*

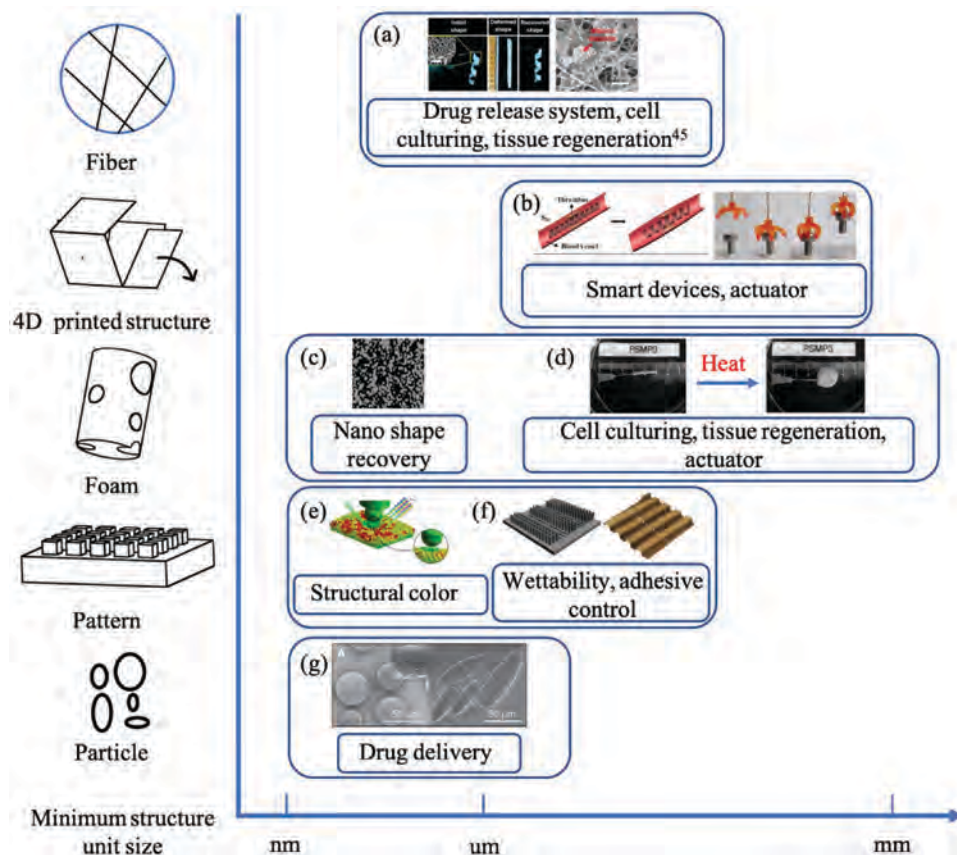


Fig. 2 SMPs with microstructure. (a) Electrospun nanofiber shape recovery process. Reproduced with permission.<sup>45</sup> Copyright 2014, American Chemical Society. (b) 4D printed SMP shape recovery process. Reproduced with permission.<sup>46,47</sup> Published under a CC-BY 4.0 license. Copyright 2016, the authors. Copyright 2017, American Chemical Society. (c) AFM topography images of the porous PGMA film, and shape recovery of SMP foam. Reproduced with permission.<sup>48</sup> Copyright 2014, The Royal Society of Chemistry. (d) Photo of the shape memory foam. Reproduced with permission.<sup>49</sup> Copyright 2013, American chemical society. (e) SMP porous structure for control of the structure color. Reproduced with permission.<sup>50</sup> Copyright 2015, American Chemical Society. (f) Rice-leaf-like structure shapes. Reproduced with permission.<sup>51</sup> Copyright 2018, Wiley-VHC. Reproduced with permission.<sup>52</sup> Copyright 2012, Wiley-VHC. (g) SEM images of particles in their permanent spherical shape (left) and programmed prolate ellipsoidal shape (right).<sup>53</sup> Copyright 2013, Wiley-VHC.

structure and the performance are different, making SMPs more widely used. However, to the best of our knowledge, there has been no new model or theory for nanostructured SMPs yet. Finite element analysis (FEA) is an effective method to characterize nano/microstructured SMPs. The micromechanical model can be combined with other models to further extend the description of polymers with nano/microstructures. It is no exaggeration to say that the introduction of stimulus-responsive materials with controllable nano/microstructures has brought about a revolution in the area of active materials. The integration of controllable nano/microstructures into one material is expected to broaden the application base for soft smart materials and structures, and offers insight into the future directions for smart devices and similar products.<sup>41–44</sup>

## 2. Shape memory polymers

SMPs exhibiting the shape memory effect (SME) depend on two phases in the chemical structure of the polymer: (1) a

switchable phase (soft molecular components) with movable and reversible chains that implement temporary shape fixing and recovery, and (2) a fixed phase (hard components) based on chemical or physical crosslinking that sets the original shape.<sup>22,54</sup> During the shape change process, the SMP is deformed into the desired shape by applying an external force when the temperature is above the transition temperature  $T_{\text{trans}}$  ( $T_g$  or  $T_m$ ), at which point the molecular chains are flexible and movable. Upon cooling below  $T_{\text{trans}}$ , the flexible chains become fixed and stress is stored in the molecular structure. Reheating once more above  $T_{\text{trans}}$ , the flexible chains once again become movable, the stress is released, and the crosslinked network points resume their original positions, resulting in the recovery of the original shape.<sup>7,55</sup>

Traditional SMPs were classified as one-way dual-SME,<sup>56</sup> meaning that there are two shape configurations, and that the transition from the original shape to the alternative temporary shape is a one-way process mediated by a single thermal cycle. Many modern applications for smart materials call for SMPs with multiple functions and multiple shapes, with three

or more shapes being necessary in some specialist applications. These multi-shape SMPs (multiple-SME) are realized through two alternative approaches: (1) a single SMP exhibiting a broad transition temperature range,<sup>57–59</sup> or (2) multicomponent polymers in which the different components have different transition temperatures.<sup>60</sup> In this way, SMPs and their composites with multiple-SME can be progressed through a sequence of shape changes using controlled thermal cycling and could subsequently revert to the original shape by reversing the sequence. Although SMPs have the advantage of remembering several different shapes, there is also a critical limitation in that SMPs cannot be automatically stepped through all of these shapes (perhaps reverting to the original shape) within a single thermal cycle. The introduction of the two-way SME solves this problem as two-way SMPs exhibit reversible shape memory behavior during the thermally-mediated shape change process.<sup>38,61,62</sup> Shape deformation occurs when the temperature exceeds  $T_{\text{trans}}$ , but when the temperature is reduced, the original shape is restored. The key point is that the SMP retains the ability to repeat this behavior indefinitely through multiple thermal cycles. The reversible SME in which SMPs respond directly to environmental conditions opens up potential applications in biomedical science and related applications.<sup>63,64</sup>

Owing to the numerous available design and fabrication options for SMPs (*e.g.* different components, different molecular weights, chemical reactions, or physical crosslinking), the physical form and behavior can be varied over a wide range, and the resulting<sup>7</sup> SMPs can be divided into numerous categories. Traditionally, SMPs are classified as thermoplastic or thermosetting polymers based on the use of chemical or physical crosslinking reactions, respectively. Describing SMPs as one-way or two-way provides a simple classification based on the programming cycle.<sup>22</sup> In addition, the actuation approach can be used to classify stimuli-responsive SMPs, for example, thermally-induced SMPs, light-activated SMPs, electrically-

driven SMPs, and water-sensitive SMPs.<sup>10</sup> In essence, all of these classifications define the basic molecular requirements and mechanisms of SMPs.

### 3. Stimulus-responsive methods

SMPs exhibit a range of attractive material properties and in recent years have been the focus of a great deal of research and development.<sup>7,10,22</sup> The means of stimulation plays a significant role for many practical applications and several modes of triggering smart polymers have been used, including heat, light, water, moisture, pH, microwaves, and electrical and magnetic fields.<sup>7,10,15</sup> Nanoscale science and technology has assumed enormous importance in obtaining the various actuation methods. Direct thermal activation was the first reported means of stimulating SMP shape change and is the most widespread and straightforward. However, the range of applications is somewhat limited by the need to control the polymers in an environment akin to an oven or water bath. Therefore, adding nanoparticles into the polymer matrix to realize indirect heating and remote control is necessary and important. Indirect heating methods such as using electrical/magnetic fields, light, and microwaves can better meet the needs of practical applications by providing an easy and convenient way of remotely activating the polymers.

Shape memory polymer composites, in which functional nanomaterials are embedded in SMP matrices (Fig. 3), offer a means for the practical realization of indirectly activated stimuli-responsive smart polymers. Popular fillers in use in different smart systems include CNTs, CB, CNFs,  $\text{Fe}_3\text{O}_4$ , SiC, Ni, Au, Ag, cellulose nanocrystals, and graphene oxide.<sup>65–70</sup> Molecular vibration in the polymer and composite systems is the key enabler for the indirect generation of heat. For example, the addition of CNTs can facilitate SMP shape change through microwave induced heating.<sup>71</sup> Other research has reported that

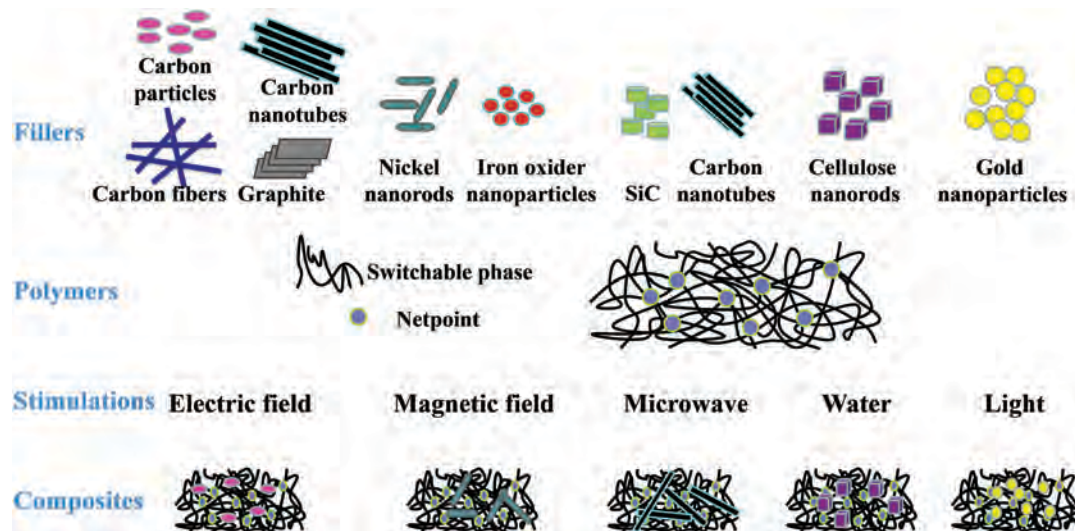


Fig. 3 Composite fillers and associated SMP activation mechanisms.

pure polycaprolactone actuated by microwaves exhibits a rapid recovery speed.<sup>14</sup> Magnetic nanoparticle fillers have also been used for the heat activation of smart polymers.<sup>72,73</sup> In such cases, the heating is induced by varying the magnetic field, and the particle size and concentration determine the magnitude of the response. For example, SMP composite films can be used to fabricate complex origami-like structures with programmable multiple shape memory properties that allow them to be magnetically activated and reconfigured into complex bent/twisted shapes or 3D boxes.<sup>74</sup>

In addition to the electromagnetic stimuli described, other activation methods with significant potential for future applications include mechanical pressure (*e.g.* finger pressure)<sup>18</sup> and sound (*e.g.* audible or ultrasound).<sup>19,75</sup> In the case of water or solvent sensitive SMPs, stimulation is possible with liquid-induced activation through direct physical swelling or chemical bonding (*e.g.* hydrogen bonds).<sup>17,76,77</sup> Moreover, the addition of organic salts to the SMP matrix can bring about water-induced shape recovery, the mechanism of which is the dissolution of the water soluble salts and the consequent creation of porous structures in the polymer.<sup>78</sup>

In addition to composites with a single dedicated activation mechanism, some research has focused on the design of composites with multiple concurrent activation mechanisms, including composites with tunable shape memory performance.<sup>79</sup> One recent example demonstrated a three-segment polystyrene-based SMP multi-composite (CNT filled, Fe<sub>3</sub>O<sub>4</sub> filled, and pure polystyrene) that exhibited a selective actuation-response in an alternating magnetic field modulated at 30 kHz and 13.56 MHz.<sup>40</sup> The potential of such materials for applications requiring complex re-configurable structures is demonstrated by this system exhibiting not only multi-mode selective activation, but also a multiple shape memory function with three separate shapes.

## 4. Nano/microstructures and morphology

With the development of nanotechnology, the research and application of nano/microstructure polymer materials have made rapid progress. New methods have been put forward constantly, and various new deductions have appeared in traditional methods. The synthesis of various methods to build multi-level and multi-scale nanostructures is used to achieve functionality and intelligence. Obtaining a specific nano/microstructure is the basis for the application of SMPs. During their early stage of development, SMPs were applied in the form of bulk polymers in most fields.<sup>7,22,23,80</sup> Gradually, nano/microstructures have emerged to fulfill the needs of a developing range of demonstrated and potential applications. Manufacturing methods that have been used to achieve the necessary nano/microstructures and shapes have included spin coating, electrospinning, transfer printing, foaming, plastic and metal molding, and 3D or 4D printing. These methods have allowed for SMP fabrication across a wide range of spatial scales from the nanoscale to the microscale, including nanofibers (Fig. 4a),<sup>81</sup> thin porous films (Fig. 4b),<sup>18</sup> surface micropatterns on SMPs (Fig. 4c),<sup>56</sup> foams with different pore morphologies (Fig. 4d),<sup>82</sup> and micro/nanoparticles (Fig. 4e).<sup>53</sup> In recent years, microscale SMPs have attracted increasing attention—particularly fibers and foams—for the surface patterning of optical devices and in biomedical engineering.<sup>32,83,84</sup>

### 4.1 Shape memory nano/microfibers

Increasingly, practical applications of SMPs call for shape memory components fabricated in a variety of complex application-specific form factors. Traditionally, common fabrication methods have included injection molding and liquid molding, which can only produce simple shapes despite the

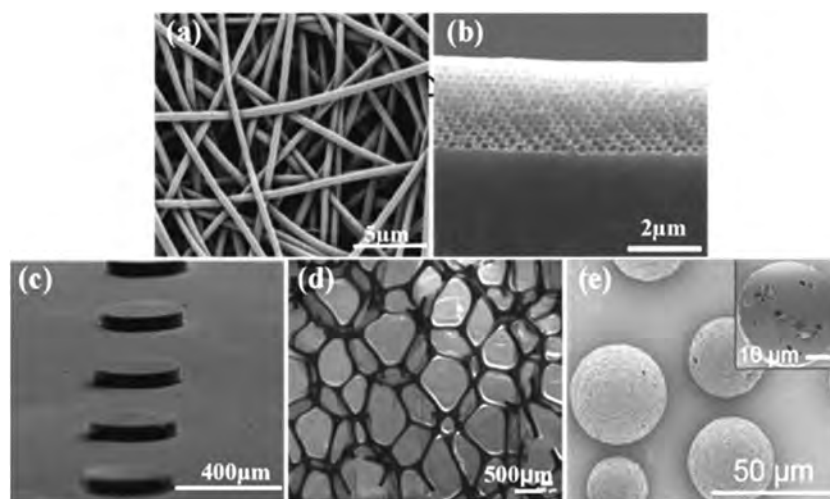


**Fig. 4** SMPs with various structures from the nanoscale to the macroscale. (a) Nanofibers. Reproduced with permission.<sup>81</sup> Published under a CC-BY 4.0 license. Copyright 2015, the authors. (b) Thin porous films. Reproduced with permission.<sup>18</sup> Published under a CC-BY 4.0 license. Copyright 2015, the authors. (c) Surface micropatterns on SMPs. Reproduced with permission.<sup>56</sup> Copyright 2015, American Chemical Society. (d) Foams with different pore morphologies. Reproduced with permission.<sup>82</sup> Copyright 2012, Wiley Periodicals, Inc. (e) Micro/nanoparticles. Reproduced with permission.<sup>53</sup> Copyright 2013, Wiley-VHC.

relative complexity of the processes. Consequently, new manufacturing methods have emerged that are better suited to the application-specific needs of shape memory components.

Electrospinning is a method to prepare nano/microfibers or particles by using a high-voltage electrostatic force. Compared with other methods to construct one-dimensional nano/micro materials, the electrospinning method is very simple, and the production efficiency is high, with excellent versatility. Therefore, in recent years, it has aroused widespread interest. Electrospinning is an established technique for the fabrication of organic or inorganic fibers with scales ranging from nanometers to micrometers and is well known as a method for preparing two dimensional (2D) and three dimensional (3D) fibrous structures.<sup>85–87</sup> The advantages of this method include simplicity, speed, controllability, and compact size, and the ability to electrospin some polymers that do not show spinning properties into fibrous structures. Currently, more than 100 polymers have been electrospun into fibers, including many shape memory polymers, such as polyurethane, polycaprolactone, polylactic acid, Nafion, and chitosan/poly(ethylene oxide).<sup>88–90</sup> In general, the ideal electrospun fibers have characteristics of a smooth surface, uniform diameter and round cross-section. Electrospun fibers can be designed with tunable secondary structures, which are usually obtained by adjusting the process parameters. SMPs and their composites can be electrospun into a variety of fibrous morphologies (Fig. 5), including non-woven fibers (Fig. 5a),<sup>91</sup> oriented fibers (Fig. 5b),<sup>92</sup> fibers with a core/shell structure (Fig. 5c),<sup>93</sup> and fibers with a functional particle filling (Fig. 5d).<sup>94</sup> Shape memory nano/microfibers show excellent shape memory performance and other specific properties by combining with some functional materials, being widely used in many fields. The adjustable high surface area and porosity of shape memory nano/microfibers can mimic the fibrillar nature of the extracellular matrix

used in tissue engineering and provide more opportunities for immobilization of functional groups in diagnostics and other applications. In addition, compared to the traditional fibrous drug delivery system, shape memory nano/microfibers used in drug delivery systems can realize more precisely controlled drug release. The co-electrospinning technique further extends the method to a greater range of polymers that includes thermosetting polymers, which can be electrospun into fibers. Zhang *et al.* extended this method to make a co-electrospun core/shell structure fiber-based composite using polycaprolactone as the shell and epoxy as the core.<sup>93</sup> Tuning of the individual properties of both components is possible with this approach, and adding epoxy enhanced the mechanical properties of the composite significantly. The resulting fibers exhibited excellent shape memory performance and have potential biomedical applications.<sup>45,95–97</sup> In addition, electrospinning of SMPs with functional particle fillers can be used to achieve composite fibers with a multi-shape memory effect and rapid on-demand actuation by an external magnetic field.<sup>74,98</sup> These properties are useful for some biomedical tissue scaffolds and drug release, and also demonstrate the potential value of such functional fillers. The different SMP nanofiber features are summarized in Table 1, including the shape recovery ratio  $R_r$  and shape fixing ratio  $R_f$ .

SMPs with fibrous structures have been particularly well-developed owing to their large surface areas, which allow for easy penetration and surface adsorption.<sup>95,96</sup> Fibers and fibrous membranes are flexible and easily deformable and offer significant potential across a range of applications that call for an active structural/functional element. In the biomedical domain, shape memory nanofibers have served as scaffolds that provide a convenient and controllable substrate for cell growth.<sup>45</sup> Typically, cells are cultured on a static surface; however, some research has demonstrated cell culture on fiber sheets with

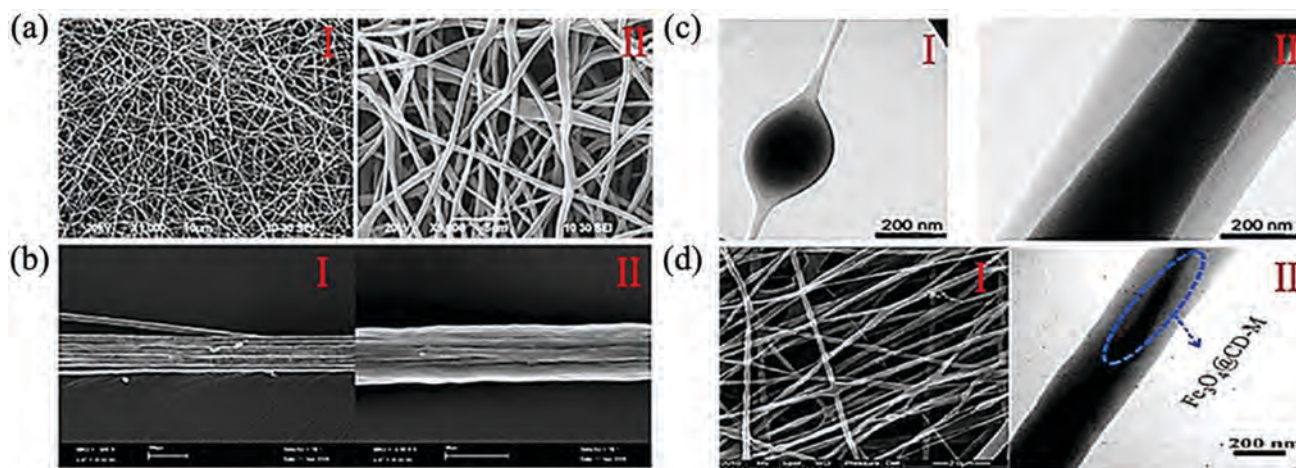


Fig. 5 Electrospinning technology used with SMPs and their composites: (a) SEM image of SMPU nonwoven nanofibers formed by multi-electrospinning. Reproduced with permission.<sup>99</sup> Copyright 2011, Springer. (b) SEM of SMF-3. View of multifilaments (500 $\times$ ). Reproduced with permission.<sup>92</sup> Copyright 2011, IOP. (c) TEM images of (I) SMPU-PUPy53 and (II) TPUPPyMDI35 core-shell nanofibers. Reproduced with permission.<sup>100</sup> Copyright 2011, eXPRESS Polymer Letters. (d) TEM image of c-PCL/Fe<sub>3</sub>O<sub>4</sub>@CD-M electrospun composite fibers. Reproduced with permission.<sup>94</sup> Copyright 2012, Elsevier.

**Table 1** The structure, material, driving condition, fiber diameter, application and research team of shape memory nano/microfibers

Shape changing material	Driving condition	Fiber diameter	$R_r$ (%)	$R_f$ (%)	Application	Research team
Nafion	130 °C heating	200–400 nm	92–94	88–92	Scaffold fabrication	Zhang <i>et al.</i> <sup>90</sup>
PCL, epoxy	70 °C heating	750–1200 nm	≈ 100	≈ 100	Smart structure	Zhang <i>et al.</i> <sup>93</sup>
PCL, CNT, Fe <sub>3</sub> O <sub>4</sub>	Magnetism	300 nm	90–92	75–84	Tissue engineering	Gong <i>et al.</i> <sup>94</sup>
PU	40 °C heating	100–500 nm	> 95	> 92	Wound healing	Tan <i>et al.</i> <sup>95</sup>
Vinylbenzyl chloride (VBC)	UV irradiation	500 nm	N/A	N/A	Controlled release	Fu <i>et al.</i> <sup>96</sup>
PDLLA-co-TMC	39 °C heating	400–1800 nm	94–98	98–99	Tissue engineering	Bao <i>et al.</i> <sup>45</sup>
PU	37 °C heating	Nanoscale	94–96	99–100	Cell differentiation	Tseng <i>et al.</i> <sup>97</sup>
Lignin	Moisture	Nanoscale	N/A	N/A	Actuator	Dallmeyer <i>et al.</i> <sup>101</sup>
PLA, polypyrrole	Electricity 30 V	1–15 μm	98	98	Actuator	Zhang <i>et al.</i> <sup>102</sup>
Poly(ω-pentadecalactone)	60 °C heating	1.8–3.1 μm	49–80	92–93	Degradable material	Matsumoto <i>et al.</i> <sup>103</sup>
Polyacrylonitrile (PAN)	Electricity 14 V	200–600 nm	≈ 100	≈ 100	Remote control	Zhang <i>et al.</i> <sup>104</sup>
PCL-PEG	Water	810 ± 28 nm	44–83	77–91	Water sensor	Gu <i>et al.</i> <sup>105</sup>
PCL	25–55 °C water	200–1000 μm	≈ 100	≈ 100	Actuator	Zhang <i>et al.</i> <sup>106</sup>
Polyferrocenylmethylvinylsilane	Electricity 1.5–2 V	2.0 ± 0.4 μm	N/A	N/A	Electric actuator	McDowell <i>et al.</i> <sup>107</sup>
PCL, PEO	55 °C heating	3–10 μm	N/A	N/A	Tissue engineering	Yao <i>et al.</i> <sup>108</sup>

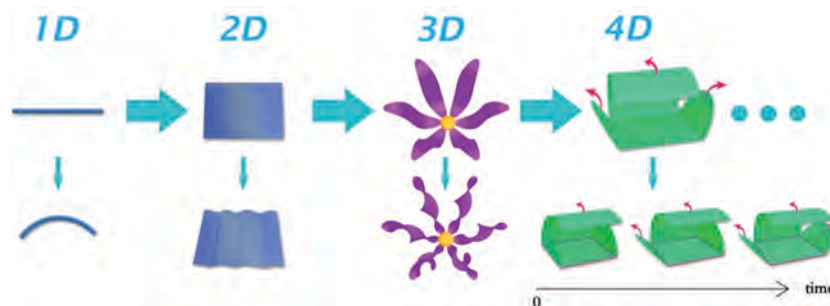
scaffolds that were programmed to change morphology during cell culture. For example, shape memory polyurethane fiber scaffolds have been used to test the hypothesis that a shape-memory-actuated change in fiber alignment can control the behavior and morphology of attached viable cells.<sup>97</sup>

#### 4.2 4D printed nano/microstructures

A 4D printed polymer is a kind of material that can transform from one shape to another separate from the print bed. Printing technologies have been widely applied in the manufacture of 1D/2D/3D/4D prototypes and products.<sup>109–113</sup> Additive manufacturing in the form of 3D printing is a process that enables the fabrication of complex 3D objects from digital data through selective 2D deposition of sequentially layered materials, effectively building up the final 3D object layer by layer from the microscale. The research of 4D printed SMPs with nano/microstructures focuses on the refined manufacturing of materials at the microscale and the corresponding shape memory effect. It is well known that regulated nano/micro dispersed structures bring good mechanical properties to the material. 4D printed microstructures enable the material to shift at the microscale, which is necessary for reversible actuators and biomedical devices. 4D printing has been used for the fabrication of various shape memory polymers including “active origami” features to realize self-folding or self-deployment functions.<sup>35,114</sup> Moreover, selective deposition of functional fillers in defined regions of the polymer can be used to implement externally-stimulated shape

actuation and recovery, facilitating remotely-triggered transformation into different 3D shapes.<sup>114</sup> Recently, shape memory PCL has been printed into 2D and 3D shapes and has potential uses in a range of flexible and responsive electronic devices including wearable electronic devices, robotics, biomedical devices, and sensors. In addition, Qi *et al.* have taken additive manufacturing to the next level by successfully developing 4D printing, which adds the extra dimension of time to traditional 3D printing with potential applications in aerospace structures, biomedical devices, and robotics.<sup>36,115</sup> Advances in manufacturing technology are spurring researchers to focus on 5D printing, which promises to meet application-specific needs by allowing printing of even more complex shapes. It is expected that advanced printing technologies from 1D to 4D, and even up to 5D or 6D, will lead to more opportunities for smart polymer-enabled products in the future (Fig. 6).

4D printed nano/microstructures can be fabricated by fused deposition modeling (FDM) and stereolithography apparatus (SLA) techniques with a resolution of up to 1 μm,<sup>116</sup> which allows for the formation of nano/microstructures such as scaffolds,<sup>117–122</sup> honeybombs,<sup>123</sup> and microballoons.<sup>124</sup> 4D printing allows the precise manipulation of structures on the macroscale. Nano/micro scaffold structures have been particularly widely studied, specifically in bioengineering, surgery, and tissue regeneration.<sup>125</sup> 4D printed microstructures are capable of promoting cell proliferation in desired arrangements.<sup>126</sup> The 4D printed shape memory nano/microstructure can be

**Fig. 6** Printing technology used with SMPs and their composites.

compressed into a small volume, which can be transferred into a wound and then expand to the original shape under different shape recovery stimuli to refill the defect region. Cells can then be cultured on the scaffold as the porous structure gives cells enough space for growth and provides sufficient specific area for nutrient exchange. The shape recovery process significantly affects the mechanical behavior of the cells seeded on the scaffold. PCL and PU are the main SMPs used in 4D printed scaffold applications owing to their low  $T_g$  values, which can be adjusted to human body temperature. Hendrikson *et al.* fabricated a polyurethane scaffold with a glass transition temperature of  $\sim 32$  °C.<sup>117</sup> The scaffold could be stretched up to 15% strain and recover the original shape under 37 °C. The cells

seeded on the scaffold were elongated after shape recovery. Miao *et al.* adopted soybean oil epoxidized acrylate, which is a natural lipid, to fabricate a micropatterned scaffold using the SLA technique.<sup>120</sup> The scaffolds showed excellent cell compatibility, and significantly improved the cardiomyogenic differentiation of stem cells. In a further study, a 4D printed neural scaffold was designed to induce stem cell differentiation during the self-morphing process.<sup>127</sup> In addition to these applications, 4D nano/micro printing can also serve as an important method in other research areas. For example, Ge *et al.* fabricated a microgripper by 4D printing epoxy resin<sup>46</sup> (Fig. 7a). Kuang *et al.* combined the self-healing technique with the 4D printing technique.<sup>123</sup> Besides, the shape transition behavior of different

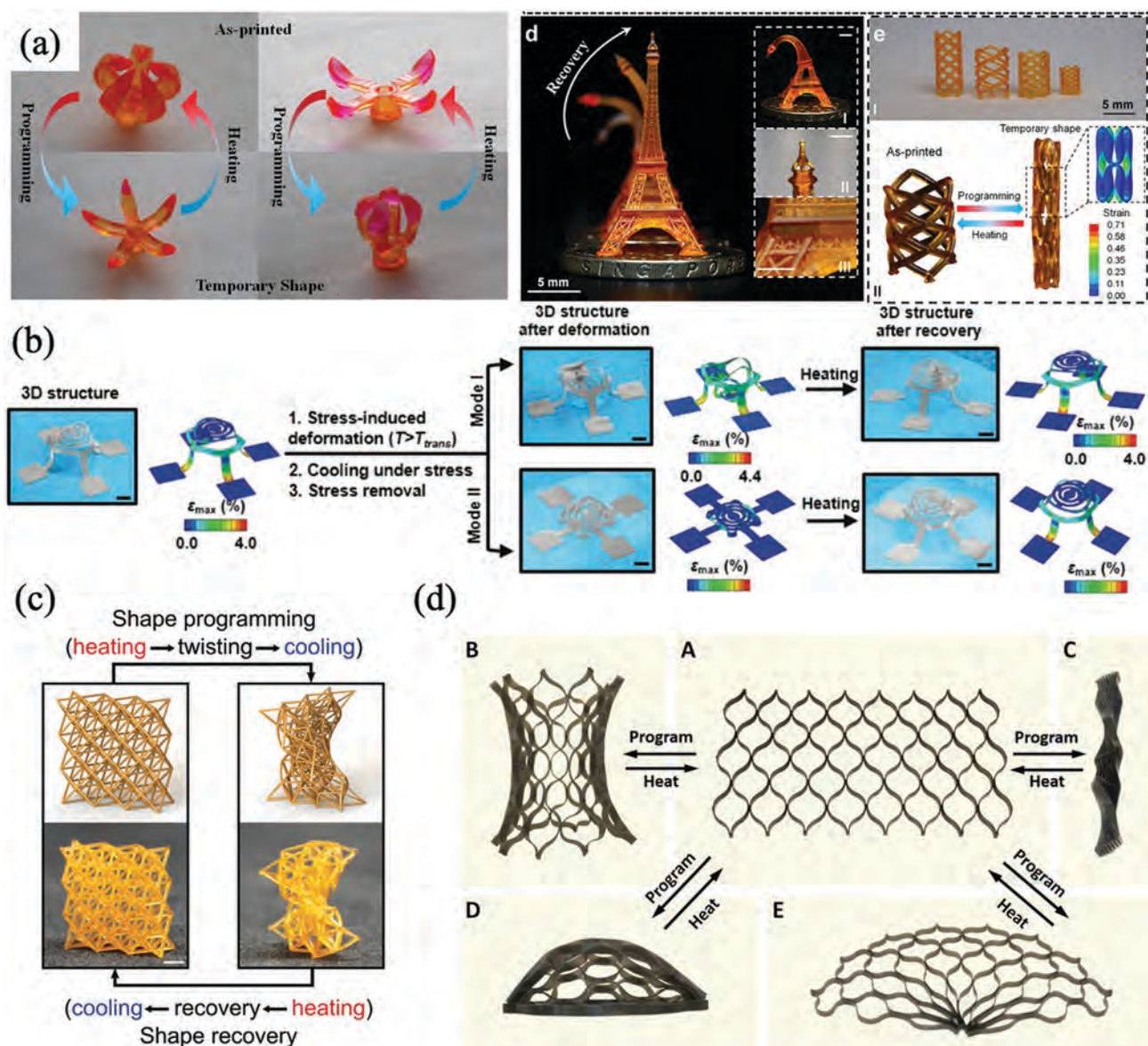


Fig. 7 Different 4D printed SMP structures. (a) 4D printed SMP shape recovery process. Reproduced with permission.<sup>46</sup> Published under a CC-BY 4.0 license. Copyright 2016, the authors. (b) 4D printed shape memory mesostructures. Reproduced with permission.<sup>128</sup> Copyright 2019, Wiley-VHC. (c) 4D printed shape memory metamaterial. Reproduced with permission.<sup>129</sup> Copyright 2019, The Royal Society of Chemistry. (d) 4D printed shape memory structure deformed from 2D to 3D. Reproduced with permission.<sup>130</sup> Published under a CC-BY 4.0 license. Copyright 2017, the authors.



deformable structures, for example, mesostructures, metamaterials, and 2D–3D transformation, has been reported<sup>128–130</sup> (Fig. 7b–d).

### 4.3 Shape changing nano/microfoams

Foam is an important conformation that has a lot of tiny holes contained inside the matrix. The unique porous structure gives the foam unique properties for insulation and compressibility. The performance of SMP foams can be tuned according to actual requirements under the remote control of shape transforming at the microscale. SMPs in the form of porous foams differ from dense bulk SMPs, benefitting from properties such as low weight and volume, self-deployability, dynamic damping capabilities, high compression ratio, simplicity, and low cost.<sup>131,132</sup> SMP foams can be fabricated using techniques such as gas blowing,<sup>133–137</sup> salt leaching,<sup>49,138–140</sup> freeze-drying,<sup>48,141,142</sup> batch blowing,<sup>143–147</sup> and microwave treatment<sup>14</sup> (Table 2). The glass transition temperature and pore size can be tuned by using different foaming methods and chemical composites. The advantages of SMP foams—including their deployable structures—show particular promise for potential applications in biomedical and aerospace engineering. For example, in bioengineering, SMP foam is an effective filling device in the surgery used to treat aneurysms.<sup>148–150</sup> In space applications, SMP foams can act as truss elements.<sup>151–153</sup>

The pore diameter of SMP foams can be on the macro or nanoscale. The micropore size distribution has a significant

effect on the shape recovery performance of the foams, and the foam density strongly influences the stress recovery properties.<sup>154</sup> When the pore size is on the macro level and it forms a hierarchical structure, the SMP foam can revert to the original shape with a higher recovery rate compared with SMP foams with a smaller pore size and a homogeneous structure. To enhance bone ingrowth, a pore size above 100  $\mu\text{m}$  was recommended.<sup>155</sup> In addition, fast triggering of the shape recovery process is important in surgery. Xie *et al.* fabricated a polyurethane/hydroxyapatite based SMP foam with a pore size above 100  $\mu\text{m}$  by polyol gas foaming<sup>133</sup> (Fig. 8a). The foam was pre-compacted to seed in the bone defect, and recovered to the original shape in saline under 40  $^{\circ}\text{C}$  in 60 s. The SMP foam showed excellent biocompatibility for bone regeneration and facilitated tissue ingrowth and neovascularization. In addition to inserting into the defect area directly, the foam can be coated on a shape memory coil and then both can be transferred to the surgery area together.<sup>156–158</sup>

Different foaming methods have diverse effects on the micro/nanopore structure. In the gas foaming method, the foaming agent leads to cell aggregation and collapse if the polymer cures for a long period. In the leaching method, the pore size is dependent on the particle size used to make the salt templates and the amount of water used for leaching the salt will affect the interconnection of the foam. The leaching method and freeze-drying method can create a pore size below

**Table 2** The structure, material, driving condition, pore diameter, application and research team of shape changing nano/micro foams

Shape changing material	Driving condition	Pore diameter	Key feature	$R_r$ (%)	$R_f$ (%)	Application	Research team
PCL	40 $^{\circ}\text{C}$ heating	670 $\mu\text{m}$	Gas blowing	91	94	Bone regeneration	Xie <i>et al.</i> <sup>133</sup>
PU	37 $^{\circ}\text{C}$ heating	40–200 $\mu\text{m}$	Gas blowing	70	N/A	Wound healing	Landsman <i>et al.</i> <sup>135</sup>
PU	37 $^{\circ}\text{C}$ heating	534–797 $\mu\text{m}$	Gas blowing	49–100	88–91	Bone defect healing	Xie <i>et al.</i> <sup>136</sup>
PU, epoxy	100 $^{\circ}\text{C}$ heating	750–1750 $\mu\text{m}$	Gas blowing	90–99	70–95	Engineering	Yao <i>et al.</i> <sup>137</sup>
<i>tert</i> -Butyl acrylate (tBA)	37 $^{\circ}\text{C}$ heating	10 $\mu\text{m}$	Salt leaching	80	N/A	Cell seeding	Wang <i>et al.</i> <sup>138</sup>
PU, urea	60 $^{\circ}\text{C}$ heating	Microscale	Salt leaching	85–99	N/A	Biomedical devices	Chai <i>et al.</i> <sup>139</sup>
PDMS, PCL	55 $^{\circ}\text{C}$ heating	200–450 $\mu\text{m}$	Salt leaching	65–100	$\approx$ 100	Biomedical devices	Zhang <i>et al.</i> <sup>49</sup>
Poly(vinyl alcohol)(PVA)	50 $^{\circ}\text{C}$ heating	60 $\mu\text{m}$	Freeze drying	45.2–100.2	109–120	Heat storage	Bonadies <i>et al.</i> <sup>141</sup>
Epoxy	55 $^{\circ}\text{C}$ heating	50–300 $\mu\text{m}$	Freeze drying	> 90	> 90	Engineering	Dong <i>et al.</i> <sup>142</sup>
Silicon	107 $^{\circ}\text{C}$ heating	10–100 nm	Freeze drying	80	N/A	Nanoscale foam	Galabura <i>et al.</i> <sup>48</sup>
PU	50 $^{\circ}\text{C}$ heating	25–75 $\mu\text{m}$	Batch blowing	67–80	99	Environment friendly material	Madbouly <i>et al.</i> <sup>144</sup>
1,6-Hexanedithiol (HDT)	100 $^{\circ}\text{C}$ heating	> 1 $\mu\text{m}$	Batch blowing	98	99.4	Insulation materials	Michal <i>et al.</i> <sup>147</sup>
PCL	Hot water, electric, microwave heating	$\approx$ 600 $\mu\text{m}$	Microwave	87.7–99.2	43–98.7	Tissue engineering	Zhang <i>et al.</i> <sup>14</sup>
PU	37 $^{\circ}\text{C}$ heating	1000 $\mu\text{m}$	Gas blowing	N/A	N/A	Biomedical devices	Rodriguez <i>et al.</i> <sup>148</sup>
Epoxy	110 $^{\circ}\text{C}$ heating	$\approx$ 200 $\mu\text{m}$	Gas blowing	72	N/A	Aerospace engineering	Santo <i>et al.</i> <sup>151,153</sup>
Epoxy/carbon nano fiber	65 $^{\circ}\text{C}$ heating	15–650 $\mu\text{m}$	Freeze drying	> 90	> 90	Engineering	Dong <i>et al.</i> <sup>159</sup>
PU, short glass fiber	80 $^{\circ}\text{C}$ heating	100–200 $\mu\text{m}$	Gas blowing	89–93	83.1–90.2	Engineering	Kausar <i>et al.</i> <sup>161</sup>
Epoxy, nano clay	120 $^{\circ}\text{C}$ heating	Microscale	Gas blowing	> 97	N/A	Engineering	Quadrini <i>et al.</i> <sup>162</sup>
Graphene, elastomer	> 48 $^{\circ}\text{C}$ , or 6–10 V heating	$\approx$ 50 $\mu\text{m}$	Freeze drying	50–99	99	Engineering	Li <i>et al.</i> <sup>167</sup>
Acrylate, methacrylate	70 $^{\circ}\text{C}$ heating	22–80 $\mu\text{m}$	Salt leaching	52–98	N/A	Engineering	Gurevitch <i>et al.</i> <sup>131</sup>

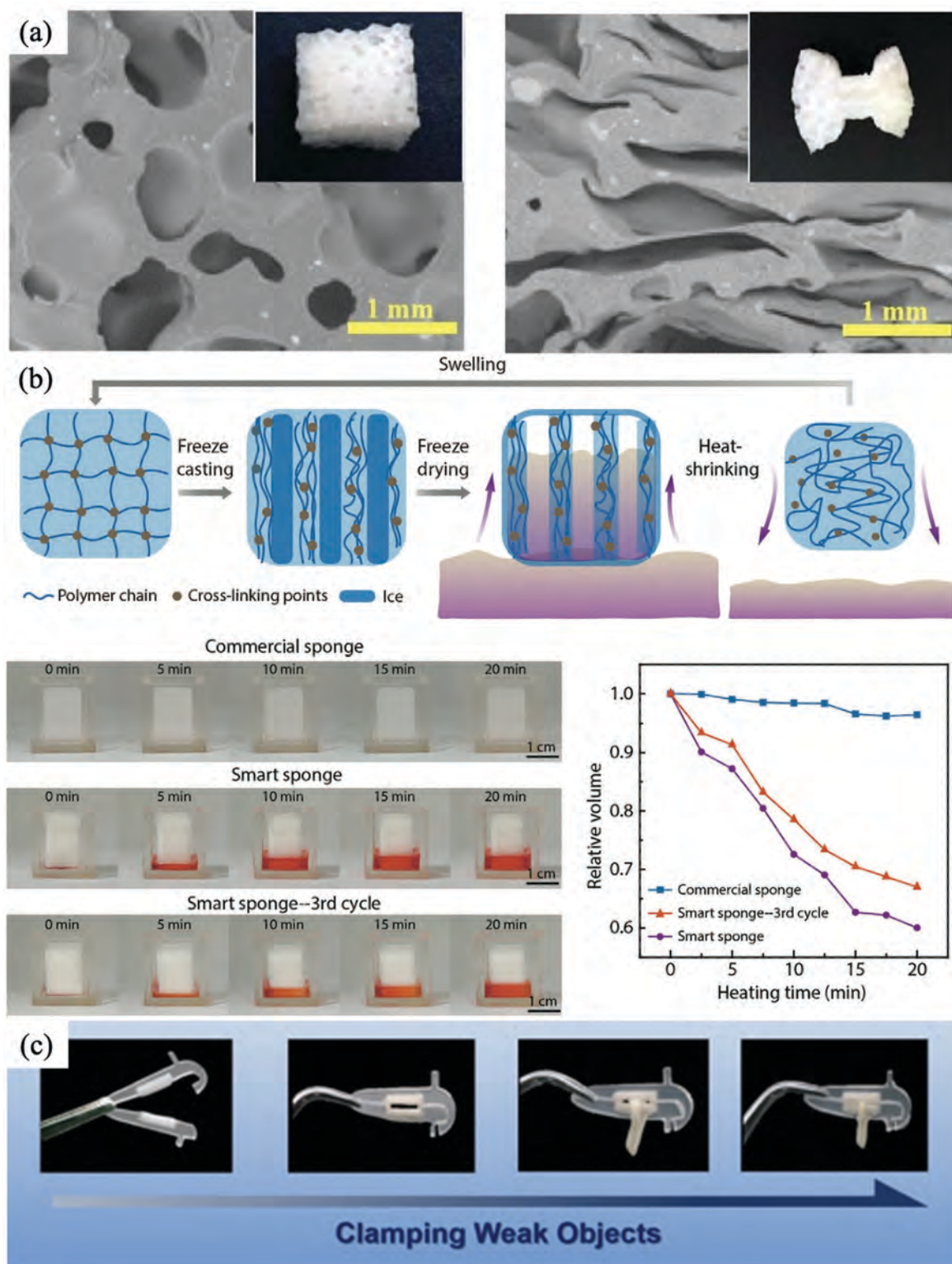


Fig. 8 SMP foam structures. (a) SMP foam microstructure before and after being compressed. Reproduced with permission.<sup>133</sup> Copyright 2018, Elsevier. (b) SMP smart foam with a thermo-responsive self-squeezing property. Reproduced with permission.<sup>168</sup> Copyright 2020, Wiley-VHC. (c) SMP clamping machine that can carry weak objects. Reproduced with permission.<sup>169</sup> Copyright 2019, American Chemical Society.

10  $\mu\text{m}$  without aggregation. Foams created by the leaching and freeze-drying methods have a more well-defined shape compared with foams synthesized using the gas blowing method.

To fabricate foams with a pore size on the nanoscale, Galabura *et al.*<sup>48</sup> demonstrated a foaming process that creates nanofoams using a freeze-drying method. When the nanofoam was

heated to 107 °C, it contracted to reach 222 nm. The nanofoam was capable of producing gradual mechanical actuation at the nanoscale.

In addition to the foaming process, micro/nanofillers have an important impact on the properties of SMP foams. For example, Dong *et al.* combined a vapor growth carbon nanotube with an epoxy foam.<sup>159</sup> The composite foam had a greater strength and a significantly higher conductivity, approaching 10 orders of magnitude higher than that of the pure epoxy foam. Hasan *et al.* incorporated aluminum oxide, silicon dioxide, and tungsten into SMP foams to tune the mechanical properties and thermal resistivity.<sup>160</sup> Kausar *et al.* combined short glass fibers with polyurethane foam to improve the mechanical performance.<sup>161</sup> Quadri *et al.* combined montmorillonite with epoxy shape memory foam to improve the compressive toughness and stress relaxation.<sup>162</sup> Piszczyk *et al.* blended graphene with polyurethane foam to improve the tensile strength and elongation.<sup>163</sup> Pearson *et al.* combined alumina, Kevlar pulp, and PBO with polyurethane foam to improve the thermostability and the storage modulus.<sup>164</sup> Liu *et al.* incorporated porous aluminum into polyurethane foam to achieve a high shape recovery ratio and a higher damping capacity.<sup>165</sup>

Other methods have also been used to enhance the properties of SMP foams. Fan *et al.* fabricated an SMP foam with a negative Poisson's ratio by steam treating.<sup>166</sup> Fan and his group modified commercial shape memory foams with a closed-cell structure based on steam penetration and condensation processes. The micro re-entrant structure formed as a result of this process is the key to creating a negative Poisson's ratio. Li *et al.* fabricated a graphene oxide aerogel foam using a vacuum/air drying method.<sup>167</sup> The uniform micro hexagon structure gave the aerogel foam a unique thermotropic shape memory performance, which resulted in excellent compressibility, a high fixing ratio, and an excellent recovery ratio. The graphene oxide foam also showed a low shape recovery actuation voltage of 6–10 V and a short recovery time of ~8 s. Cui *et al.* developed a thermally induced self-squeezing sponge with a shape memory property. The smart sponge was capable of absorbing liquid rapidly with micro aligned hollow channels, and shrinking out the absorbed liquid during heating (Fig. 8b).<sup>168</sup> In another study, Hou *et al.* constructed a clamping foam machine that can work under 50 °C (Fig. 8c).<sup>169</sup> The features of a variety of SMP foams have been summarized in Table 2.

#### 4.4 Smart nano/micropatterns

The surface nano/microstructures of polymer materials are closely related to the properties of materials. The nano/microstructures, combined with the vibrant and colorful characteristics of polymer materials, have essential scientific significance and application value in materials science, microelectronics and cell biology. SMP nano/micropatterns are uniformly distributed protrusion structures on the SMP surface. The addition of microstructure on SMP surfaces expands the range of potential applications for these unique materials. The molecular principle of SMPs does not vary with scale: micro and

nanoscale SMP microstructures exhibit properties that are identical to those of macroscale bulk SMPs and enable a diverse range of innovative applications based on “smart surfaces” with switchable properties. SMP nano/micro array structures that are capable of optical wave-front shaping are implemented in optical waveguides and passive optical devices to alter the phase of the light propagating through them. This adjustable characteristic can be used in beam splitters, color rendering, anti-counterfeiting, filtering and other functional devices. SMPs with smart nano/micropatterns can be created by nano-indentation or replica molding. Instead of altering the surface chemistry, these processes change the surface topography, which results in SMPs having unique properties. Examples include wrinkled surfaces, surfaces with controlled wetting, reversible dry adhesives, and switchable information carriers (*e.g.* 2D barcodes), as well as surfaces with controllable and changeable optical behavior. The template method can adjust the shape, structure, size and arrangement of the surface by using the confinement of the template itself and the interaction between the template and the polymer. The construction of polymer surface nano/microstructures has developed from simple replication to various flexible applications, which can build three-dimensional multi-level and multi-scale micro nanostructures.

SMP pillar arrays are common structures in smart nano/micropatterns.<sup>170–172</sup> The pillars can be shaped as cylinders, cuboids, prisms, cones and polyhedra depending on the mold structure, and are on the macroscale with a dense arrangement on the SMP surface. Altering the arrangement and size of the pillar array significantly affects the topography of the SMP surface, which induces anisotropic liquid wetting. Above the glass transition temperature the pillars contract or tilt and revert to the original shape under stimulation. This process can lead to the smart controllability of the liquid. For example, Chen *et al.* investigated the wettability of SMP pillar arrays made with epoxy resin (Fig. 9a).<sup>173</sup> The droplets on the surface adopted Wenzel state wetting in a static environment and were fully immobilized on the inclined surface. Chen and his group also described the behavior of droplets with the Cassie–Baxter model. Following the work of Chen and co-workers, Cheng *et al.* achieved the control of droplet motion on a hydrophobic surface.<sup>51</sup> By controlling the SMP pillar shape recovery behavior on the microscale, Cheng and his group created a repeatable switch between superhydrophobic isotropic and anisotropic SMP pillar arrays. Controlling the tilt angle was the key factor in realizing this behavior. The distinct topography between the SMP pillars in different states induces the transportation of the droplets. In addition to controlling the movement, Lv *et al.* investigated an approach for fabricating an SMP pillar array with tunable adhesive superhydrophobicity.<sup>174</sup> When the space between the pillars was greater than 20 μm, the SMP arrays showed low adhesion superhydrophobicity. High adhesion superhydrophobicity was achieved when a pit pillar structure was applied.

SMP porous surfaces are another important structure in smart nano/micropatterns. SMP porous surface structure can

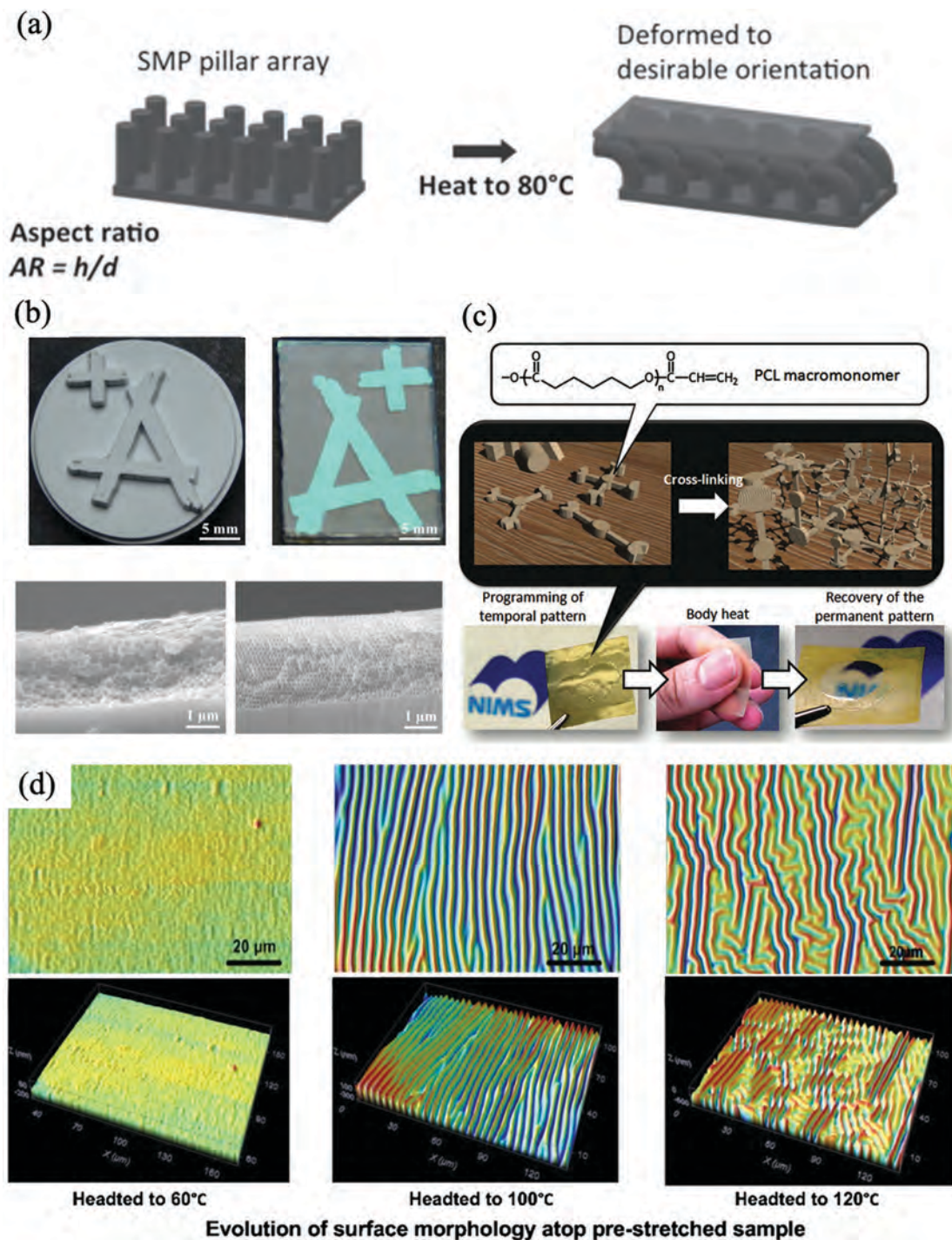


Fig. 9 SMP patterns. (a) SMP pillar array. Reproduced with permission.<sup>173</sup> Copyright 2014, Wiley-VHC. (b) SMP porous structure for control of the structure color. Reproduced with permission.<sup>50</sup> Copyright 2015, The American Chemical Society. (c) SMP wrinkled surface for altering the transmittance. Reproduced with permission.<sup>52</sup> Copyright 2012, Wiley-VHC. (d) SMP wrinkled surface for control of the structure color. Reproduced with permission.<sup>176</sup> Copyright 2011, IOP.

be fabricated by silica templating. The porous layer thickness and pore diameter affect the refraction and reflection of light. By controlling the structure deformation behavior, the color of SMP porous surfaces can be changed under different shape stimuli. Espinha *et al.* fabricated an SMP porous membrane that changed transparency under deformation<sup>175</sup> as a result of the samples

narrowing in the direction orthogonal to the stretching axis during elongation. Fang *et al.* investigated rewritable photonic patterns based on shape memory inverse opals (Fig. 9b).<sup>50</sup> A porous multi-layer structure with a diameter of approximately 200–400 nm was fabricated. Different micropatterns were written onto the SMP co-polymer membrane with a 1 mm diameter spherical sapphire tip.

In addition, wrinkled SMP surfaces can be fabricated by pressure indentation on SMP surfaces above the transition temperature with pre-stretching of the SMP, followed by surface metal coating. As the SMP recovers the original shape below a certain temperature, the metal contracts and forms a wrinkled structure. When the wavelength of these wrinkles is on the macroscale, structural color is exhibited at the surface of the material. Ebara *et al.* extended the wrinkle wavelength to the nanoscale, which created a wrinkle pattern that became transparent at human body temperature (Fig. 9c).<sup>52</sup> Zhao *et al.* investigated the structural color of different wrinkle patterns on SMP surfaces (Fig. 9d).<sup>176</sup> A 10-nm gold layer was coated on the polyurethane surface by sputter deposition. The result shows that the wrinkle degree strongly depends on the properties of the thin gold layer and the SMP substrate, which creates different wrinkle patterns. Different SMP pattern features are given in Table 3. The surface and interface are the windows to realize the function of devices and materials. The construction of surface nano/microstructures is of great significance to the performance of materials.

#### 4.5 Smart nano/microparticles

Nanoscale and microscale devices are increasingly required to support the trend towards miniaturization, for example, for use as switchable carriers for drug delivery or in brain surgery. As drug carriers, nano/microparticles have the advantages of high targeting, controlled drug release, and improved drug dissolution and absorption. The deformation performance of nano/microparticles is the same as that of macrostructured SMPs, which is determined by the SME of the material itself. Shape memory particles on the nanoscale and microscale have been reported over the past few years.<sup>78,169</sup> Yang *et al.* presented the first example of shape memory nanoparticles with an intrinsic non-spherical shape.<sup>169</sup> The fabricated nanoparticles were ellipsoidal in shape with high aspect ratio, and the shape could be controlled and manipulated by changing the underlying nematic order. The shape morphology and changing process are shown in Fig. 10a–d. Later, Wischke *et al.* prepared a kind of SMP microscale particle using an oil-in-water (o/w) emulsion technique as shown in Fig. 10e and f.<sup>78</sup> In further research, crosslinked polyester microparticles were synthesized, and the corresponding shape recovery behavior was captured and analyzed with a microelectromechanical systems (MEMS) microgripper.<sup>179</sup> The microscale particles could be

activated on demand, switching between spherical and different predefined non-spherical shapes, which enabled the tailoring of the biodistribution and biorecognition in drug delivery.

## 5. Applications

SMPs with the ability to change shape in response to external stimuli offer enormous promise and have attracted intense interest from researchers in many fields.<sup>5,8,26,109</sup> Over the past few years, SMPs of various types have been researched and developed, some of which are now commercially available. In addition to their scientific appeal, such polymers have huge potential in fields as diverse as aerospace (*e.g.* self-deployable sun sails on spacecraft), automobiles (*e.g.* intelligent bumpers), medical devices (*e.g.* surgical implants; intelligent drug delivery and release), robotics, flexible electronic devices (*e.g.* flexible mobile phones), tactile user interfaces (*e.g.* smart braille keypads), information carriers (*e.g.* 2D barcodes), and smart textiles<sup>5,29,32,35,37,38</sup> (Fig. 11). These examples represent only some of the potential opportunities, but regardless of the SMP type, structure, and size, cleverly designed SMPs promise superior performance for a wide range of practical applications.

In the aerospace sector, SMPs and their composites are already well developed. An increasing number of deployable and morphing structures have been designed and tested, including deployable optical systems, trusses, hinges, deployable mirrors, booms, flexible reflectors, antennae, solar arrays, and morphing skins.<sup>5,29,30,110</sup> In particular, SMP-based deployment devices can overcome some of the drawbacks of traditional deployable structures, notably the complex assembly processes and large sizes. Moreover, high-performance fiber reinforced SMP composites will increasingly replace traditional aerospace materials. A number of established finite element models have been developed to analyze the deformation and strain of the flexural or bending shell. It can be expected that SMPs and their composites will continue to deliver novel technologies that meet the challenging needs of the aerospace sector.

In addition to aerospace, recent development in smart polymer technologies is rapidly extending to reach other fields. SMPs in the form of fibers, yarns, and fabrics can be used to make smart textiles, clothing, and related products.<sup>32</sup> SMP fibers with tunable shape and transition temperature can be used to make responsive clothing with superior elasticity and

**Table 3** The structure, material, driving condition, minimum structure unit, application and research team of smart nano/micropatterns

Shape changing material	Driving condition	Minimum unit size	Key feature	Application	Research team
Epoxy	80 °C heating	10 μm	Replica molding	Microfluidic devices	Chen <i>et al.</i> <sup>173</sup>
Epoxy	120 °C heating	10 μm	Replica molding	Microfluidic devices	Cheng <i>et al.</i> <sup>51</sup>
Epoxy	120 °C heating	10 μm	Replica molding	Microreaction	Lv <i>et al.</i> <sup>174</sup>
Poly(1,12-dodecanediol-co-citrate)	30 °C heating	140 ± 30 nm	Replica molding	Biophotonics	Romanov <i>et al.</i> <sup>175</sup>
Polyethylene glycol (600)	Contact pressure	200–400 nm	Molding	Rewritable data storage	Fang <i>et al.</i> <sup>50</sup>
PS, PU	80–100 °C heating	700 nm	Sputter deposition	Wrinkle surfaces	Zhao <i>et al.</i> <sup>176</sup>
PCL	37 °C body heat	300 nm	Nanopattern molding	Biomaterials	Ebara <i>et al.</i> <sup>52</sup>
PS	90 °C heating	600 nm	Nano imprinting	Photonic devices	Li <i>et al.</i> <sup>177</sup>
PEG-PCL	35–41 °C heating	10–15 μm	Micro imprinting	Vessel repair	Gong <i>et al.</i> <sup>178</sup>

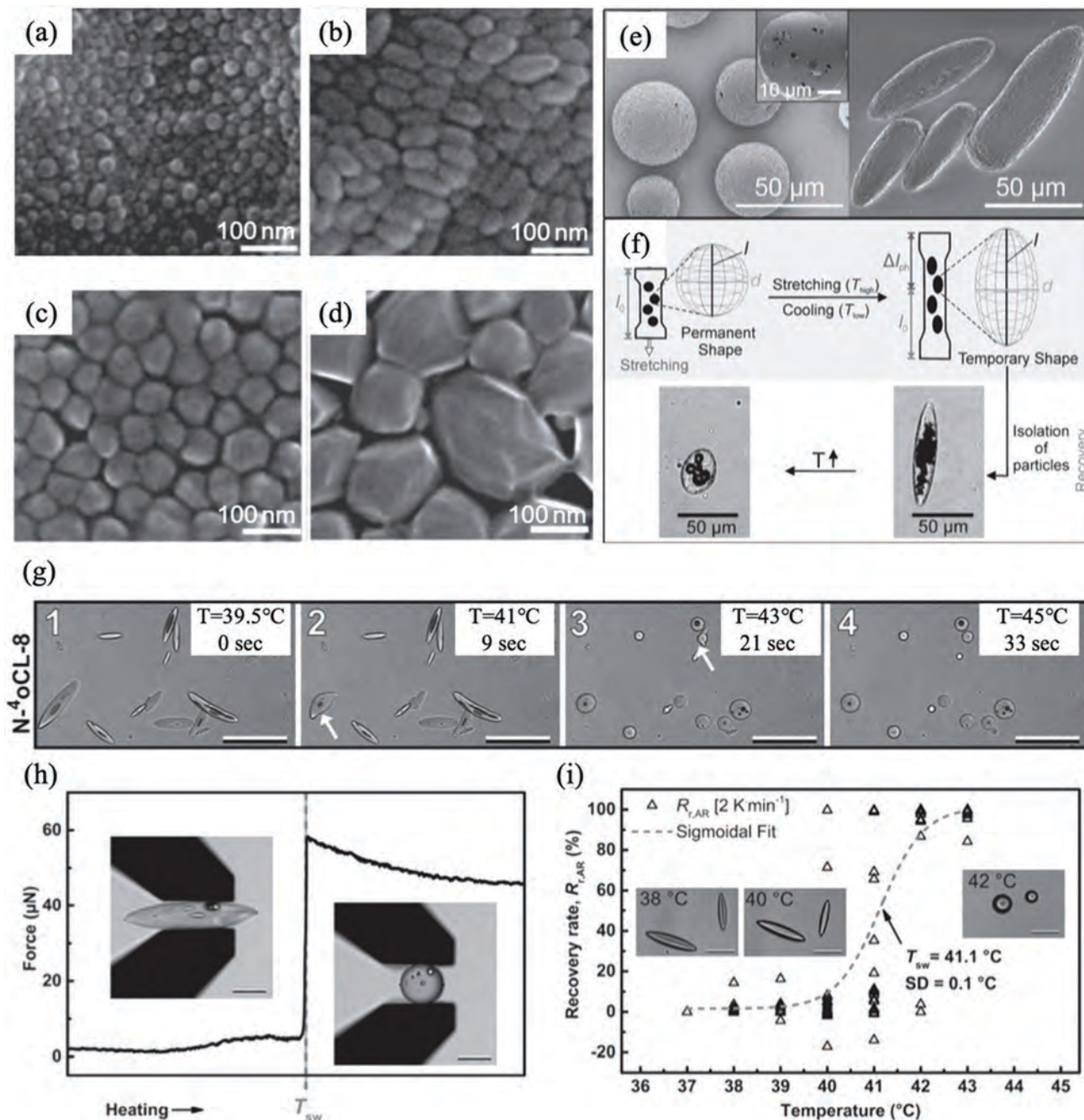


**Fig. 10** SMP particles, the apparent trend of the shape dependence on particle size confirms that seen in MCLCP: the F8BT nanoparticle shape changes from (a) spheres (30 nm) to (b) ellipsoids and back to (c) spheres (70 nm), the aspect ratio varies from 1.0 to 2.2 and back to 1.0 correspondingly; (d) irregular particles with size greater than 120 nm. Reproduced with permission.<sup>180</sup> Copyright 2005, Nature Materials. (e) SEM images of particles in their permanent spherical shape (left) and programmed prolate ellipsoidal shape (right); (f) programming of spherical particles (permanent shape) embedded in PVA phantoms to their temporary shape, and microscopy of temperature-induced shape recovery for isolated particles. Reproduced with permission.<sup>53</sup> Copyright 2013, Wiley-VHC. (g) Shape switching of polyester microparticles in an aqueous suspension. (h) Microparticles were captured and analyzed by a MEMS microgripper. (i) Analysis of the shape recovery rate for microparticles in an aqueous suspension. Reproduced with permission.<sup>179</sup> Copyright 2014, Wiley-VHC.

fit that spontaneously adjusts to the environment. In the biomedical space, biocompatible polymers, particularly polyurethane-based SMPs, have achieved excellent results and have been used in drug delivery systems, smart surgical sutures, and microactuators for blood clot removal, among other applications.<sup>28,37,38</sup> In the

automotive field, BMW is rethinking the design of automobile body shells, introducing non-metal materials to show a symbiotic relationship between materials, function, and aesthetics. SMPs offer a great deal of potential for such projects. Given the pace of innovation, SMPs will inevitably continue to play an important role

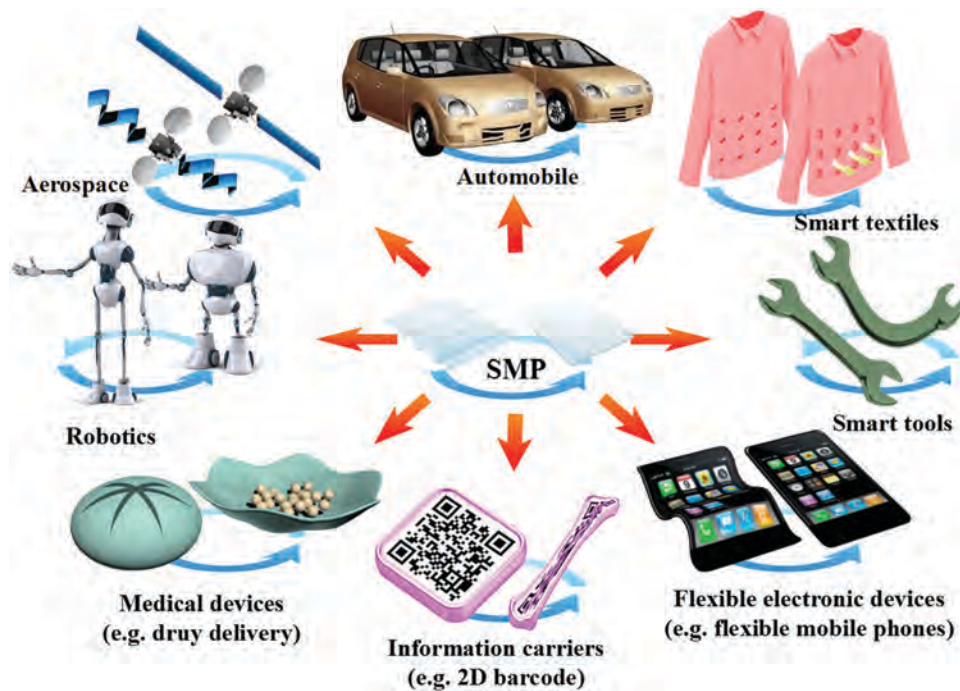


Fig. 11 Applications of SMPs and their composites in daily life.

in the development of new technologies for biomedical engineering. In addition to the chemical composition and macrostructure, the performance of the material surface depends largely on the nano/microstructure of the surface. The construction of polymer surface micro nanostructures has very important significance and application prospects in wettability regulation, thin surface optical performance enhancement, microfluidic transport and control, controlled drug release, preparation of tissue engineering materials and micro-electronic devices, *etc.* Potential applications of smart polymers will also continue to expand in other areas. SMPs have been proposed for applications as diverse as airflow control, optical devices, self-healing devices, and self-folding/self-deployable devices.<sup>30,33,36,111,112</sup>

## 6. Conclusions and outlook

As archetypal smart materials, it is apparent that SMPs can have an impact on almost every aspect of our lives. However, there are also some problems to overcome in SMP materials, structures, properties and applications. Firstly, manufacturing technologies are necessary to be developed for making different forms so that the unique structures and properties of SMPs can be exploited from the nanoscale to the macroscale. Development in manufacturing technologies, notably 4D/5D printing technology, is simplifying the SMP production process and enabling accelerated fabrication of complex shapes and structures. In the future, SMP-based products will feature ever more in our daily lives and although SMPs are already available in a variety of forms, increasingly demanding applications call for

continuous innovation. SMPs with new forms and functionality will continue to be required, for example, usability considerations lead to a need for SMPs with transition temperatures that are well matched to the particular application, while environmental considerations necessitate easily degradable “green materials” that minimize pollution. In addition, the ultimate goal is materials that are soft and flexible yet have variable stiffness, which is used for smart wearable devices and soft robotics. Most importantly, biodegradable and biocompatible SMPs with low transition temperature should be fabricated into nano or microstructures and realize remote actuation. In the biomedical sphere, SMPs and their composites show significant potential for use in tissue engineering and implanted organs that help to sustain and prolong life. Crucially, these fabrication technologies are integrating prior planning and programming of the shape memory functionality into the production process to realize SMP parts with tunable operation and remotely controlled actuation. Ultimately, it is possible to envisage soft robots with integrated sensors and actuators that can deform in response to external conditions, while still performing their predefined functions.

Moreover, deep understanding of biological mechanisms should be investigated to make more stimulus-responsive SMPs for applications. The wide range of potential applications for SMPs is underpinned by their exotic characteristics, including the multiple shape memory effect, reversible response, selective stimulus-response, and programmable shape change. Significant inspiration could be gained from the study of similar biological systems in living organisms, such as morphing skins and structures that reconfigure themselves in response to their surroundings. A thorough understanding of the underlying

biological mechanisms will bring insight to new stimulus-response technologies and their effective translation into engineered systems. SMPs offer a path to the practical realization of such complex multi-function structures and materials and chart a path towards the technologically advanced intelligent systems of the future. Based on the research of existing methods, how to construct polymer nano/microstructures on a smaller scale, with more extensive area and more accurately, and how to realize functional and intelligent polymer materials through multi-level nano/microstructures, will still be the challenges and opportunities in this field.

## Conflicts of interest

There are no conflicts to declare.

## Acknowledgements

This work is funded by the National Natural Science Foundation of China (Grant No. 11632005, 11672086, 11802075). This work was also supported by the China Postdoctoral Science Foundation funded project.

## References

- R. Vaia and J. Baur, *Science*, 2008, **319**, 420–421.
- Y. Sun and Z. Guo, *Nanoscale Horiz.*, 2019, **4**, 52–76.
- D. A. Giannakoudakis, Y. Hu, M. Florent and T. J. Bandosz, *Nanoscale Horiz.*, 2017, **2**, 356–364.
- M. Ma, L. Guo, D. G. Anderson and R. Langer, *Science*, 2013, **339**, 186–189.
- R. M. Erb, J. S. Sander, R. Grisch and A. R. Studart, *Nat. Commun.*, 2013, **4**, 1712.
- C. S. Haines, M. D. Lima, N. Li, G. M. Spinks, J. Foroughi, J. D. W. Madden, S. H. Kim, S. Fang, M. Jung de Andrade, F. Göktepe, Ö. Göktepe, S. M. Mirvakili, S. Naficy, X. Lepró, J. Oh, M. E. Kozlov, S. J. Kim, X. Xu, B. J. Swedlove, G. G. Wallace and R. H. Baughman, *Science*, 2014, **343**, 868.
- J. Leng, X. Lan, Y. Liu and S. Du, *Prog. Mater. Sci.*, 2011, **56**, 1077–1135.
- C. M. Yakacki, *Polym. Rev.*, 2013, **53**, 1–5.
- J. J. McDowell, N. S. Zacharia, D. Puzzo, I. Manners and G. A. Ozin, *J. Am. Chem. Soc.*, 2010, **132**, 3236–3237.
- H. Meng and G. Li, *Polymer*, 2013, **54**, 2199–2221.
- S. Chen, J. Hu, H. Zhuo, C. Yuen and L. Chan, *Polymer*, 2010, **51**, 240–248.
- A. Lendlein, H. Jiang, O. Jünger and R. Langer, *Nature*, 2005, **434**, 879.
- X. J. Han, Z. Q. Dong, M. M. Fan, Y. Liu, J. H. Li, Y. F. Wang, Q. J. Yuan, B. J. Li and S. Zhang, *Macromol. Rapid Commun.*, 2012, **33**, 1055–1060.
- F. Zhang, T. Zhou, Y. Liu and J. Leng, *Sci. Rep.*, 2015, **5**, 11152.
- Y. Liu, H. Lv, X. Lan, J. Leng and S. Du, *Compos. Sci. Technol.*, 2009, **69**, 2064–2068.
- M. Y. Razzaq, M. Behl and A. Lendlein, *Adv. Funct. Mater.*, 2012, **22**, 184–191.
- W. M. Huang, B. Yang, L. An, C. Li and Y. S. Chan, *Appl. Phys. Lett.*, 2005, **86**, 114105.
- Y. Fang, Y. Ni, S.-Y. Leo, C. Taylor, V. Basile and P. Jiang, *Nat. Commun.*, 2015, **6**, 7416.
- G. Li, G. Fei, H. Xia, J. Han and Y. Zhao, *J. Mater. Chem.*, 2012, **22**, 7692–7696.
- Y. Fang, Y. Ni, B. Choi, S. Y. Leo, J. Gao, B. Ge, C. Taylor, V. Basile and P. Jiang, *Adv. Mater.*, 2015, **27**, 3696–3704.
- W. M. Huang, B. Yang, Y. Zhao and Z. Ding, *J. Mater. Chem.*, 2010, **20**, 3367–3381.
- Q. Zhao, H. J. Qi and T. Xie, *Prog. Polym. Sci.*, 2015, **49–50**, 79–120.
- Q. Meng and J. Hu, *Composites, Part A*, 2009, **40**, 1661–1672.
- A. Lendlein and R. Langer, *Science*, 2002, **296**, 1673–1676.
- Y. Liu, H. Du, L. Liu and J. Leng, *Smart Mater. Struct.*, 2014, **23**.
- W. M. Sokolowski and S. C. Tan, *J. Spacecr. Rockets*, 2007, **44**, 750–754.
- A. Khaldi, C. Plesse, F. Vidal and S. K. Smoukov, *Adv. Mater.*, 2015, **27**, 4418–4422.
- H. Jinlian, M. Harper, L. Guoqiang and I. I. Samuel, *Smart Mater. Struct.*, 2012, **21**, 053001.
- X. Luo and P. T. Mather, *ACS Macro Lett.*, 2013, **2**, 152–156.
- H. Lu, W. Min Huang, X. Lian Wu, Y. Chun Ge, F. Zhang, Y. Zhao and J. Geng, Heating/ethanol-response of poly methyl methacrylate (PMMA) with gradient pre-deformation and potential temperature sensor and anti-counterfeit applications, 2014.
- T. Pretsch, M. Ecker, M. Schildhauer and M. Maskos, *J. Mater. Chem.*, 2012, **22**, 7757–7766.
- H. Xu, C. Yu, S. Wang, V. Malyarchuk, T. Xie and J. A. Rogers, *Adv. Funct. Mater.*, 2013, **23**, 3299–3306.
- I. V. W. Small, P. Singhal, T. S. Wilson and D. J. Maitland, *J. Mater. Chem.*, 2010, **20**, 3356–3366.
- A. G. A. Coombes, S. C. Rizzi, M. Williamson, J. E. Barralet, S. Downes and W. A. Wallace, *Biomaterials*, 2004, **25**, 315–325.
- Y. Mao, K. Yu, M. S. Isakov, J. Wu, M. L. Dunn and H. Jerry Qi, *Sci. Rep.*, 2015, **5**, 13616.
- Q. Ge, H. J. Qi and M. L. Dunn, *Appl. Phys. Lett.*, 2013, **103**, 131901.
- A. S. Gladman, E. A. Matsumoto, R. G. Nuzzo, L. Mahadevan and J. A. Lewis, *Nat. Mater.*, 2016, **15**, 413–418.
- T. Chung, A. Romo-Uribe and P. T. Mather, *Macromolecules*, 2008, **41**, 184–192.
- Y. Wu, J. Hu, C. Zhang, J. Han, Y. Wang and B. Kumar, *J. Mater. Chem. A*, 2015, **3**, 97–100.
- W. Li, Y. Liu and J. Leng, *J. Mater. Chem. A*, 2015, **3**, 24532–24539.
- Z. Pei, Y. Yang, Q. Chen, Y. Wei and Y. Ji, *Adv. Mater.*, 2016, **28**, 156–160.
- H. Koerner, G. Price, N. A. Pearce, M. Alexander and R. A. Vaia, *Nat. Mater.*, 2004, **3**, 115–120.
- X. Luo and P. T. Mather, *Adv. Funct. Mater.*, 2010, **20**, 2649–2656.



- 44 M. D. Hager, S. Bode, C. Weber and U. S. Schubert, *Prog. Polym. Sci.*, 2015, **49-50**, 3–33.
- 45 M. Bao, X. Lou, Q. Zhou, W. Dong, H. Yuan and Y. Zhang, *ACS Appl. Mater. Interfaces*, 2014, **6**, 2611–2621.
- 46 Q. Ge, A. H. Sakhaei, H. Lee, C. K. Dunn, N. X. Fang and M. L. Dunn, *Sci. Rep.*, 2016, **6**, 31110.
- 47 H. Wei, Q. Zhang, Y. Yao, L. Liu, Y. Liu and J. Leng, *ACS Appl. Mater. Interfaces*, 2017, **9**, 876–883.
- 48 Y. Galabura, A. P. Soliani, J. Giammarco, B. Zdyrko and I. Luzinov, *Soft Matter*, 2014, **10**, 2567–2573.
- 49 D. Zhang, K. M. Petersen and M. A. Grunlan, *ACS Appl. Mater. Interfaces*, 2013, **5**, 186–191.
- 50 Y. Fang, Y. Ni, S. Y. Leo, B. Wang, V. Basile, C. Taylor and P. Jiang, *ACS Appl. Mater. Interfaces*, 2015, **7**, 23650–23659.
- 51 Z. Cheng, D. Zhang, T. Lv, H. Lai, E. Zhang, H. Kang, Y. Wang, P. Liu, Y. Liu, Y. Du, S. Dou and L. Jiang, *Adv. Funct. Mater.*, 2018, **28**, 1705002.
- 52 M. Ebara, K. Uto, N. Idota, J. M. Hoffman and T. Aoyagi, *Adv. Mater.*, 2012, **24**, 273–278.
- 53 C. Wischke, M. Schossig and A. Lendlein, *Small*, 2014, **10**, 83–87.
- 54 A. Lendlein and S. Kelch, *Angew. Chem., Int. Ed.*, 2002, **41**, 2034–2057.
- 55 K. Yu, Q. Ge and H. J. Qi, *Nat. Commun.*, 2014, **5**, 3066.
- 56 J. Wang, J. Li, N. Li, X. Guo, L. He, X. Cao, W. Zhang, R. He, Z. Qian, Y. Cao and Y. Chen, *Chem. Mater.*, 2015, **27**, 2439–2448.
- 57 T. Xie, *Nature*, 2010, **464**, 267–270.
- 58 P. Miaudet, A. Derré, M. Maugey, C. Zakri, P. M. Piccione, R. Inoubli and P. Poulin, *Science*, 2007, **318**, 1294.
- 59 Y. Bai, X. Zhang, Q. Wang and T. Wang, Shape memory property of microcrystalline cellulose–poly( $\epsilon$ -caprolactone) polymer network with broad transition temperature, 2014.
- 60 J. Zotzmann, M. Behl, D. Hofmann and A. Lendlein, *Adv. Mater.*, 2010, **22**, 3424–3429.
- 61 R. M. Baker, J. H. Henderson and P. T. Mather, *J. Mater. Chem. B*, 2013, **1**, 4916–4920.
- 62 I. Kolesov, O. Dolynchuk, D. Jehnichen, U. Reuter, M. Stamm and H.-J. Radosch, *Macromolecules*, 2015, **48**, 4438–4450.
- 63 S. Pandini, T. Riccò, A. Borboni, I. Bodini, D. Vetturi, D. Cambiaghi, M. Toselli, K. Paderni, M. Messori, F. Pilati, F. Chiellini and C. Bartoli, *J. Mater. Eng. Perform.*, 2014, **23**, 2545–2552.
- 64 C. A. Tippetts, Q. Li, Y. Fu, E. U. Donev, J. Zhou, S. A. Turner, A.-M. S. Jackson, V. S. Ashby, S. S. Sheiko and R. Lopez, *ACS Appl. Mater. Interfaces*, 2015, **7**, 14288–14293.
- 65 H. Lu, J. Gou, J. Leng and S. Du, *Appl. Phys. Lett.*, 2011, **98**, 174105.
- 66 G. P. Tandon, K. Goecke, K. Cable and J. Baur, *J. Intell. Mater. Syst. Struct.*, 2010, **21**, 1365–1381.
- 67 L. Haibao, L. Fei, G. Jihua, L. Jinsong and D. Shanyi, *Smart Mater. Struct.*, 2014, **23**, 085034.
- 68 M. Yoonessi, Y. Shi, D. A. Scheiman, M. Lebron-Colon, D. M. Tigelaar, R. A. Weiss and M. A. Meador, *ACS Nano*, 2012, **6**, 7644–7655.
- 69 H. Du, Z. Song, J. Wang, Z. Liang, Y. Shen and F. You, *Sens. Actuators, A*, 2015, **228**, 1–8.
- 70 L. Tan, L. Gan, J. Hu, Y. Zhu and J. Han, *Composites, Part A*, 2015, **76**, 115–123.
- 71 K. Yu, Y. Liu and J. Leng, *RSC Adv.*, 2014, **4**, 2961–2968.
- 72 U. N. Kumar, K. Kratz, M. Heuchel, M. Behl and A. Lendlein, *Adv. Mater.*, 2011, **23**, 4157–4162.
- 73 R. Mohr, K. Kratz, T. Weigel, M. Lucka-Gabor, M. Moneke and A. Lendlein, *Proc. Natl. Acad. Sci. U. S. A.*, 2006, **103**, 3540.
- 74 F. H. Zhang, Z. C. Zhang, C. J. Luo, I. T. Lin, Y. Liu, J. Leng and S. K. Smoukov, *J. Mater. Chem. C*, 2015, **3**, 11290–11293.
- 75 G. Li, Q. Yan, H. Xia and Y. Zhao, *ACS Appl. Mater. Interfaces*, 2015, **7**, 12067–12073.
- 76 H. Lu, J. Leng and S. Du, *Soft Matter*, 2013, **9**, 3851–3858.
- 77 R. Xiao, J. Guo, D. L. Safranski and T. D. Nguyen, *Soft Matter*, 2015, **11**, 3977–3985.
- 78 W. Wang, H. Lu, Y. Liu and J. Leng, *J. Mater. Chem. A*, 2014, **2**, 5441–5449.
- 79 Z. He, N. Satarkar, T. Xie, Y.-T. Cheng and J. Z. Hilt, *Adv. Mater.*, 2011, **23**, 3192–3196.
- 80 Y. Wang, Y. Zhu, J. Huang, J. Cai, J. Zhu, X. Yang, J. Shen and C. Li, *Nanoscale Horiz.*, 2017, **2**, 225–232.
- 81 S. Jiang, F. Liu, A. Lerch, L. Ionov and S. Agarwal, *Adv. Mater.*, 2015, **27**, 4865–4870.
- 82 P. Singhal, J. N. Rodriguez, W. Small, S. Egleston, J. Van de Water, D. J. Maitland and T. S. Wilson, *J. Polym. Sci., Part B: Polym. Phys.*, 2012, **50**, 724–737.
- 83 D. Zhang, W. L. Burkes, C. A. Schoener and M. A. Grunlan, *Polymer*, 2012, **53**, 2935–2941.
- 84 S. A. Bencherif, R. W. Sands, D. Bhatta, P. Arany, C. S. Verbeke, D. A. Edwards and D. J. Mooney, *Proc. Natl. Acad. Sci. U. S. A.*, 2012, **109**, 19590–19595.
- 85 D. Li and Y. Xia, *Adv. Mater.*, 2004, **16**, 1151–1170.
- 86 Z.-M. Huang, Y. Z. Zhang, M. Kotaki and S. Ramakrishna, *Compos. Sci. Technol.*, 2003, **63**, 2223–2253.
- 87 M. Hecht, B. Soberats, J. Zhu, V. Stepanenko, S. Agarwal, A. Greiner and F. Würthner, *Nanoscale Horiz.*, 2019, **4**, 169–174.
- 88 D. I. Cha, H. Y. Kim, K. H. Lee, Y. C. Jung, J. W. Cho and B. C. Chun, *J. Appl. Polym. Sci.*, 2005, **96**, 460–465.
- 89 H. Zhuo, J. Hu and S. Chen, *Mater. Lett.*, 2008, **62**, 2074–2076.
- 90 F. Zhang, Z. Zhang, Y. Liu and J. Leng, *Fibers Polym.*, 2014, **15**, 534–539.
- 91 H. Chen, X. Cao, J. Zhang, J. Zhang, Y. Ma, G. Shi, Y. Ke, D. Tong and L. Jiang, *J. Mater. Chem.*, 2012, **22**, 22387–22391.
- 92 J. FengLong, Z. Yong, H. JinLian, L. Yan, Y. Lap-Yan and Y. GuangDou, *Smart Mater. Struct.*, 2006, **15**, 1547.
- 93 F. Zhang, Z. Zhang, Y. Liu, W. Cheng, Y. Huang and J. Leng, *Composites, Part A*, 2015, **76**, 54–61.
- 94 T. Gong, W. Li, H. Chen, L. Wang, S. Shao and S. Zhou, *Acta Biomater.*, 2012, **8**, 1248–1259.
- 95 L. Tan, J. Hu, H. Huang, J. Han and H. Hu, *Int. J. Biol. Macromol.*, 2015, **79**, 469–476.

- 96 G.-D. Fu, L.-Q. Xu, F. Yao, G.-L. Li and E.-T. Kang, *ACS Appl. Mater. Interfaces*, 2009, **1**, 2424–2427.
- 97 L.-F. Tseng, P. T. Mather and J. H. Henderson, *Acta Biomater.*, 2013, **9**, 8790–8801.
- 98 F. Zhang, Z. Zhang, Y. Liu, H. Lu and J. Leng, *Smart Mater. Struct.*, 2013, **22**.
- 99 H. T. Zhuo, J. L. Hu and S. J. Chen, *J. Mater. Sci.*, 2011, **46**, 3464–3469.
- 100 H. T. Zhuo, J. L. Hu and S. J. Chen, *eXPRESS Polym. Lett.*, 2011, **5**, 182–187.
- 101 I. Dallmeyer, S. Chowdhury and J. F. Kadla, *Biomacromolecules*, 2013, **14**, 2354–2363.
- 102 F. Zhang, Y. Xia, L. Wang, L. Liu, Y. Liu and J. Leng, *ACS Appl. Mater. Interfaces*, 2018, **10**(41), 35526–35532, DOI: 10.1021/acsami.8b12743.
- 103 H. Matsumoto, T. Ishiguro, Y. Konosu, M. Minagawa, A. Tanioka, K. Richau, K. Kratz and A. Lendlein, *Eur. Polym. J.*, 2012, **48**, 1866–1874.
- 104 F. Zhang, Z. Zhang, Y. Liu and J. Leng, *Smart Mater. Struct.*, 2014, **23**, 065020.
- 105 X. Z. Gu and P. T. Mather, *RSC Adv.*, 2013, **3**, 15783–15791.
- 106 J. N. Zhang, Y. M. Ma, J. J. Zhang, D. Xu, Q. L. Yang, J. G. Guan, X. Y. Cao and L. Jiang, *Mater. Lett.*, 2011, **65**, 3639–3642.
- 107 J. J. McDowell, N. S. Zacharia, D. Puzzo, I. Manners and G. A. Ozin, *J. Am. Chem. Soc.*, 2010, **132**, 3236–3237.
- 108 Y. T. Yao, H. Q. Wei, J. J. Wang, H. B. Lu, J. S. Leng and D. Hui, *Composites, Part B*, 2015, **83**, 264–269.
- 109 H. Wei, Q. Zhang, Y. Yao, L. Liu, Y. Liu and J. Leng, *ACS Appl. Mater. Interfaces*, 2017, **9**, 876–883.
- 110 F. Momeni, S. M. Mehdi Hassani, N. X. Liu and J. Ni, *Mater. Des.*, 2017, **122**, 42–79.
- 111 S. Tibbits, *Archit. Des.*, 2014, **84**, 116–121.
- 112 Y. Zhang, L. Shi, D. Hu, S. Chen, S. Xie, Y. Lu, Y. Cao, Z. Zhu, L. Jin, B.-O. Guan, S. Rogge and X. Li, *Nanoscale Horiz.*, 2019, **4**, 601–609.
- 113 S. Deng, J. Wu, M. D. Dickey, Q. Zhao and T. Xie, *Adv. Mater.*, 2019, **31**, 1903970.
- 114 K. Yu, A. Ritchie, Y. Mao, M. L. Dunn and H. J. Qi, *Procedia IUTAM*, 2015, **12**, 193–203.
- 115 Q. Ge, C. K. Dunn, H. J. Qi and M. L. Dunn, *Smart Mater. Struct.*, 2014, **23**.
- 116 C. Sun, N. Fang, D. M. Wu and X. Zhang, *Sens. Actuators, A*, 2005, **121**, 113–120.
- 117 W. J. Hendrikson, J. Rouwkema, F. Clementi, C. A. van Blitterswijk, S. Fare and L. Moroni, *Biofabrication*, 2017, **9**, 031001.
- 118 W. J. Hendrikson, J. Rouwkema, C. A. van Blitterswijk and L. Moroni, *RSC Adv.*, 2015, **5**, 54510–54516.
- 119 S. Miao, W. Zhu, N. J. Castro, M. Nowicki, X. Zhou, H. Cui, J. P. Fisher and L. G. Zhang, *Sci. Rep.*, 2016, **6**, 27226.
- 120 S. Miao, H. Cui, M. Nowicki, S.-J. Lee, J. Almeida, X. Zhou, W. Zhu, X. Yao, F. Masood, M. W. Plesniak, M. Mohiuddin and L. G. Zhang, *Biofabrication*, 2018, **10**.
- 121 S. Sharifi, S. Blanquer and D. W. Grijpma, *J. Appl. Biomater. Funct. Mater.*, 2012, **10**, 280–286.
- 122 B. Zhang, J. D. Skelly, J. R. Maalouf, D. C. Ayers and J. Song, *Sci. Transl. Med.*, 2019, **11**, eaau7411.
- 123 X. Kuang, K. Chen, C. K. Dunn, J. Wu, V. C. F. Li and H. J. Qi, *ACS Appl. Mater. Interfaces*, 2018, **10**, 7381–7388.
- 124 A. S. Wu, W. Small Iv, T. M. Bryson, E. Cheng, T. R. Metz, S. E. Schulze, E. B. Duoss and T. S. Wilson, *Sci. Rep.*, 2017, **7**, 4664.
- 125 C. Lin, J. Lv, Y. Li, F. Zhang, J. Li, Y. Liu, L. Liu and J. Leng, *Adv. Funct. Mater.*, 2019, **29**, 1906569.
- 126 D. Liu, T. Xiang, T. Gong, T. Tian, X. Liu and S. Zhou, *ACS Appl. Mater. Interfaces*, 2017, **9**, 19725–19735.
- 127 S. Miao, H. Cui, T. Esworthy, B. Mahadik, S.-J. Lee, X. Zhou, S. Y. Hann, J. P. Fisher and L. G. Zhang, *Adv. Sci.*, 2020, **7**, 1902403.
- 128 X. Wang, X. Guo, J. Ye, N. Zheng, P. Kohli, D. Choi, Y. Zhang, Z. Xie, Q. Zhang, H. Luan, K. Nan, B. H. Kim, Y. Xu, X. Shan, W. Bai, R. Sun, Z. Wang, H. Jang, F. Zhang, Y. Ma, Z. Xu, X. Feng, T. Xie, Y. Huang, Y. Zhang and J. A. Rogers, *Adv. Mater.*, 2019, **31**, 1805615.
- 129 C. Yang, M. Boorugu, A. Dopp, J. Ren, R. Martin, D. Han, W. Choi and H. Lee, *Mater. Horiz.*, 2019, **6**, 1244–1250.
- 130 Z. Ding, C. Yuan, X. Peng, T. Wang, H. J. Qi and M. L. Dunn, *Sci. Adv.*, 2017, **3**, e1602890.
- 131 I. Gurevitch and M. S. Silverstein, *Soft Matter*, 2012, **8**.
- 132 D. Khedaoui, C. Boisson, F. D'Agosto and D. Montarnal, *Angew. Chem., Int. Ed.*, 2019, **58**, 15883–15889.
- 133 R. Xie, J. Hu, O. Hoffmann, Y. Zhang, F. Ng, T. Qin and X. Guo, *Biochim. Biophys. Acta, Gen. Subj.*, 2018, **1862**, 936–945.
- 134 S. M. Kang, S. J. Lee and B. K. Kim, *eXPRESS Polym. Lett.*, 2012, **6**, 63–69.
- 135 T. L. Landsman, T. Touchet, S. M. Hasan, C. Smith, B. Russell, J. Rivera, D. J. Maitland and E. Cosgriff-Hernandez, *Acta Biomater.*, 2017, **47**, 91–99.
- 136 R. Xie, J. Hu, F. Ng, L. Tan, T. Qin, M. Zhang and X. Guo, *Ceram. Int.*, 2017, **43**, 4794–4802.
- 137 Y. Yao, T. Zhou, C. Yang, Y. Liu and J. Leng, *Smart Mater. Struct.*, 2016, **25**.
- 138 J. Wang, M. E. Brasch, R. M. Baker, L. F. Tseng, A. N. Pena and J. H. Henderson, *J. Mater. Sci.: Mater. Med.*, 2017, **28**, 151.
- 139 Q. Chai, Y. Huang, T. L. Kirley and N. Ayres, *Polym. Chem.*, 2017, **8**, 5039–5048.
- 140 J. D. Erndt-Marino, D. J. Munoz-Pinto, S. Samavedi, A. C. Jimenez-Vergara, P. Diaz-Rodriguez, L. Woodard, D. Zhang, M. A. Grunlan and M. S. Hahn, *ACS Biomater. Sci. Eng.*, 2015, **1**, 1220–1230.
- 141 I. Bonadies, A. Izzo Renzi, M. Cocca, M. Avella, C. Carfagna and P. Persico, *Ind. Eng. Chem. Res.*, 2015, **54**, 9342–9350.
- 142 Y. Dong, Y. Fu and Q.-Q. Ni, *J. Appl. Polym. Sci.*, 2015, **132**, 42599.
- 143 M. Karimi, M. Heuchel, T. Weigel, M. Schossig, D. Hofmann and A. Lendlein, *J. Supercrit. Fluids*, 2012, **61**, 175–190.
- 144 S. A. Madbouly and A. Lendlein, *Macromol. Mater. Eng.*, 2012, **297**, 1213–1224.

- 145 L. Meng, H. Liu, L. Yu, S. Khalid, L. Chen, T. Jiang and Q. Li, *J. Appl. Polym. Sci.*, 2017, **134**.
- 146 H.-Y. Mi, X. Jing, M. R. Salick, X.-F. Peng and L.-S. Turng, *Polym. Eng. Sci.*, 2014, **54**, 2947–2957.
- 147 B. T. Michal, W. A. Brenn, B. N. Nguyen, L. S. McCorkle, M. A. B. Meador and S. J. Rowan, *Chem. Mater.*, 2016, **28**, 2341–2347.
- 148 J. N. Rodriguez, M. W. Miller, A. Boyle, J. Horn, C. K. Yang, T. S. Wilson, J. M. Ortega, W. Small, L. Nash, H. Skoog and D. J. Maitland, *J. Mech. Behav. Biomed. Mater.*, 2014, **40**, 102–114.
- 149 J. N. Rodriguez, Y. J. Yu, M. W. Miller, T. S. Wilson, J. Hartman, F. J. Clubb, B. Gentry and D. J. Maitland, *Ann. Biomed. Eng.*, 2012, **40**, 883–897.
- 150 J. M. Ortega, J. Hartman, J. N. Rodriguez and D. J. Maitland, *Ann. Biomed. Eng.*, 2013, **41**, 725–743.
- 151 L. Santo, F. Quadrini, G. Mascetti, F. Dolce and V. Zolesi, *Acta Astronaut.*, 2013, **91**, 333–340.
- 152 Q. Fabrizio, S. Loredana and S. E. Anna, *Mater. Lett.*, 2012, **69**, 20–23.
- 153 L. Santo, F. Quadrini, W. Villadei, G. Mascetti and V. Zolesi, *Procedia Eng.*, 2015, **104**, 50–56.
- 154 T. Sauter, K. Kratz and A. Lendlein, *Macromol. Chem. Phys.*, 2013, **214**, 1184–1188.
- 155 A. C. Jones, C. H. Arns, A. P. Sheppard, D. W. Huttmacher, B. K. Milthorpe and M. A. Knackstedt, *Biomaterials*, 2007, **28**, 2491–2504.
- 156 A. J. Boyle, T. L. Landsman, M. A. Wierzbicki, L. D. Nash, W. Hwang, M. W. Miller, E. Tuzun, S. M. Hasan and D. J. Maitland, *J. Biomed. Mater. Res., Part B*, 2016, **104**, 1407–1415.
- 157 A. J. Boyle, M. A. Wierzbicki, S. Herting, A. C. Weems, A. Nathan, W. Hwang and D. J. Maitland, *Med. Eng. Phys.*, 2017, **49**, 56–62.
- 158 J. Horn, W. Hwang, S. L. Jessen, B. K. Keller, M. W. Miller, E. Tuzun, J. Hartman, F. J. Clubb, Jr. and D. J. Maitland, *J. Biomed. Mater. Res., Part B*, 2017, **105**, 1892–1905.
- 159 Y. Dong, J. Ding, J. Wang, X. Fu, H. Hu, S. Li, H. Yang, C. Xu, M. Du and Y. Fu, *Compos. Sci. Technol.*, 2013, **76**, 8–13.
- 160 S. M. Hasan, R. S. Thompson, H. Emery, A. L. Nathan, A. C. Weems, F. Zhou, M. B. Monroe and D. J. Maitland, *RSC Adv.*, 2016, **6**, 918–927.
- 161 A. Kausar, *J. Polym. Eng.*, 2018, **38**, 33–40.
- 162 F. Quadrini, L. Santo and E. A. Squeo, *Polym.-Plast. Technol. Eng.*, 2012, **51**, 560–567.
- 163 Ł. Piszczyk, M. Strankowski and P. Kosmela, *Polym. Compos.*, 2017, **38**, 2248–2253.
- 164 A. Pearson and H. E. Naguib, *Composites, Part B*, 2017, **122**, 192–201.
- 165 S. Liu, A. Li, S. He and P. Xuan, *Composites, Part A*, 2015, **78**, 35–41.
- 166 D. Fan, M. Li, J. Qiu, H. Xing, Z. Jiang and T. Tang, *ACS Appl. Mater. Interfaces*, 2018, **10**, 22669–22677.
- 167 C. Li, L. Qiu, B. Zhang, D. Li and C. Y. Liu, *Adv. Mater.*, 2016, **28**, 1510–1516.
- 168 Y. Cui, Y. Wang, Z. Shao, A. Mao, W. Gao and H. Bai, *Adv. Mater.*, 2020, **32**, 1908249.
- 169 Y. Hou, G. Fang, Y. Jiang, H. Song, Y. Zhang and Q. Zhao, *ACS Appl. Mater. Interfaces*, 2019, **11**, 32423–32430.
- 170 C. Li, Y. Jiao, X. Lv, S. Wu, C. Chen, Y. Zhang, J. Li, Y. Hu, D. Wu and J. Chu, *ACS Appl. Mater. Interfaces*, 2020, **12**, 13464–13472.
- 171 H.-Y. Tseng, Y.-H. Chen, R.-Y. Chen and H. Yang, *ACS Appl. Mater. Interfaces*, 2020, **12**, 10883–10892.
- 172 Y. Liu, M. Y. Razzaq, T. Rudolph, L. Fang, K. Kratz and A. Lendlein, *Macromolecules*, 2017, **50**, 2518–2527.
- 173 C. M. Chen and S. Yang, *Adv. Mater.*, 2014, **26**, 1283–1288.
- 174 T. Lv, Z. Cheng, D. Zhang, E. Zhang, Q. Zhao, Y. Liu and L. Jiang, *ACS Nano*, 2016, **10**(10), 9379–9386, DOI: 10.1021/acsnano.6b04257.
- 175 S. G. Romanov, G. Lozano, D. Gerace, C. Monat, H. R. Míguez, A. Espinha, M. Concepción Serrano, Á. Blanco and C. López, presented in part at the Photonic Crystal Materials and Devices XI, 2014.
- 176 Y. Zhao, W. M. Huang and Y. Q. Fu, *J. Micromech. Microeng.*, 2011, **21**, 067007.
- 177 P. Li, Y. Han, W. Wang, Y. Liu, P. Jin and J. Leng, *Sci. Rep.*, 2017, **7**, 44333.
- 178 T. Gong, K. Zhao, X. Liu, L. Lu, D. Liu and S. Zhou, *Small*, 2016, **12**, 5769–5778.
- 179 F. Friess, U. Nöchel, A. Lendlein and C. Wischke, *Adv. Healthcare Mater.*, 2014, **3**, 1986–1990.
- 180 Z. Yang, W. T. Huck, S. M. Clarke, A. R. Tajbakhsh and E. M. Terentjev, *Nat. Mater.*, 2005, **4**, 486–490.